120

BioRadiations

A Resource for Life Science Research

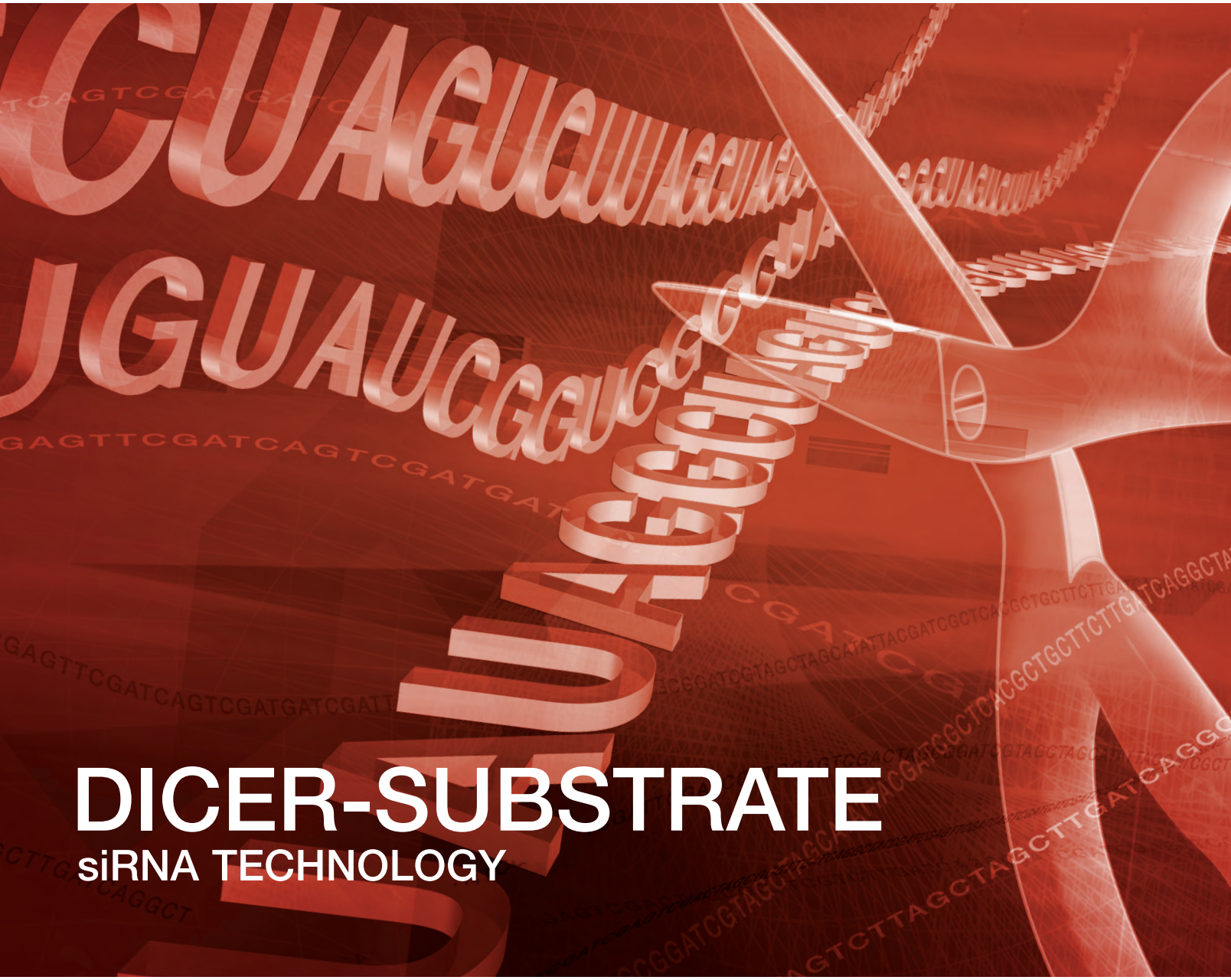

DICER-SUBSTRATE
siRNA TECHNOLOGY

In this issue:

BIO-RAD

New siLentMer™ siRNA!
Check out our new validated and predesigned 27-mer siRNA duplexes

Bio-Rad and RNAi. Come have a look.

From design to detection, Bio-Rad supports your RNAi research.

With a broad range of proven delivery technologies, award-winning detection systems, and a suite of high-quality support products, it's clear that Bio-Rad has a vision for RNAi.

- High-performing potent siRNA for ≥85% knockdown with as low as 5 nM siRNA
- Greatest choice of delivery technologies
- RNA and protein purification products
- Automated microfluidic RNA analysis
- Sensitive, optimized cDNA synthesis kits
- Systems for protein and mRNA detection

For a close look at Bio-Rad's tools for RNAi, visit us on the Web at **www.bio-rad.com/RNAi/**

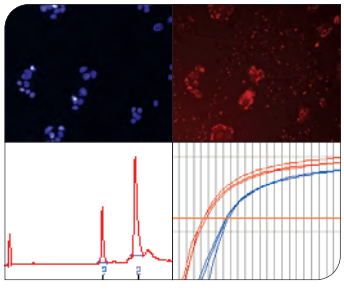

MCF-7 cells transfected using siLentFect™ reagent. RNA purified and analyzed using the Aurum™ total RNA kit and Experion™ system. Real-time PCR detection performed using iScript™ cDNA synthesis kit.

BIO-RAD SUBSIDIARY
TELEPHONE NUMBERS

Australia 61-2-9914-2800
Austria 43-1-877-89-01
Belgium 32-9-385-55-11
Brazil 55-21-3237-9400
Canada 905-712-2771
China 86-21-6426-0808
Czech Republic 420-241-430-532
Denmark 45-44-52-10-00
Finland 358-9-804-22-00
France 33-1-47-95-69-65
Germany 49-89-318-84-0
Hong Kong 852-2-789-3300
Hungary 36-1-455-8800
India 91-124-402-9300
Israel 03-963-6050
Italy 39-06-5295892
Japan 81-3-5811-6270
Korea 82-2-3473-4460
Latin America 00-1-305-894-5950
Mexico 55-52-00-05-20
The Netherlands 31-318-540666
New Zealand 64-9-415-2280
Norway 47-23-38-41-30
Poland 48-22-331-99-99
Portugal 351-21-472-7700
Russia 7-095-721-14-04
Singapore 65-6415-3188
South Africa 27-861-246-723
Spain 34-91-590-5200
Sweden 46-8-555-12700
Switzerland 41-61-717-9555
Taiwan 88-62-2578-7189
Thailand 662-651-8311
United Kingdom 44-20-8328-2000
USA Toll free 1-800-4BIORAD
(1-800-424-6723)

discover.bio-rad.com

On the cover:
Conceptual illustration by
Chris Crutchfield

BioRadiations magazine is published by
Bio-Rad Laboratories, Inc.
2000 Alfred Nobel Drive
Hercules, CA 94547 USA

If you have comments or suggestions regarding BioRadiations, please e-mail us at **bioradiations@bio-rad.com**

BioRadiations

issue 120, 2006

TO OUR READERS

Gene silencing via RNA interference (RNAi) is a powerful tool for studying gene function. One of the challenges facing researchers using this tool has been to silence the gene of interest without activating a general immune response that shuts down all protein synthesis in the cell. Our feature this month describes the development of siLentMer™ Dicer-substrate small interfering RNAs (siRNAs), which enter the RNAi pathway earlier than other siRNAs and thus are more potent and specific mediators of RNAi.

COVER STORY

DEPARTMENTS

DIMENSIONS

TECHNICAL REPORTS

Legal Notices — See page 32.

Beacon Designer Software Version 5.10

Primer Design Software for PCR and Real-Time PCR Applications

Beacon Designer software designs optimized probes (TaqMan, molecular beacons, or LNA) and primer sets for single and multiplex PCR and allelic discrimination assays. Unlimited technical support is included and is available via telephone, e-mail, or fax.

Multiplex Assay Development

Beacon Designer software uses innovative proprietary algorithms to design the optimum primer and probe sets for multiplex experiments (Figure 1). You can analyze up to four different sequences for a single reaction. You can even design primer and probe sets that are compatible with predesigned sets from publications or your prior work. Beacon Designer software allows you to load hundreds of single-nucleotide polymorphisms (SNPs) to design probes for multiplex assays. This powerful software program first designs approximately 50 probes and primers for each sequence. Each designed primer and probe set is then verified against every other to minimize melting temperature (T_m) mismatches and cross-hybridization.

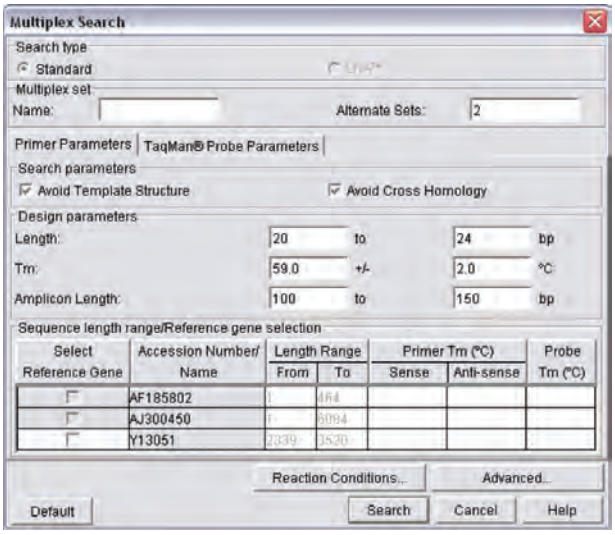

Fig. 1. Beacon Designer software's multiplex search window.

Time Savings

Beacon Designer software is fast and easy to use. Its unique capability to directly access several different databases and automatically incorporate and analyze the information into project files produces quality results quickly (Figure 2). Beacon Designer software connects with the mfold server to check for secondary structure, connects with BLAST to search for primer homology, and finishes its analysis to provide the best primer design in only 5 minutes. Furthermore, sequences can be opened directly from Entrez, dbSNP, or files saved on your local hard drive.

Superior Results

Beacon Designer software searches templates to avoid regions that form stable secondary structures at annealing and extension temperatures. The presence of stable secondary structures reduces PCR yields and hence hinders the quantification process. The secondary structure search, combined with the BLAST search using local or public databases, automatically designs primers free of both inter- and intra-sequence homologies.

Beacon Designer software scans the specified sequence and provides all possible oligonucleotides by calculating various sequence properties. The software uses default parameters that have been selected based on extensive research. Beacon Designer probes and primers produce robust, highly specific PCR amplifications.

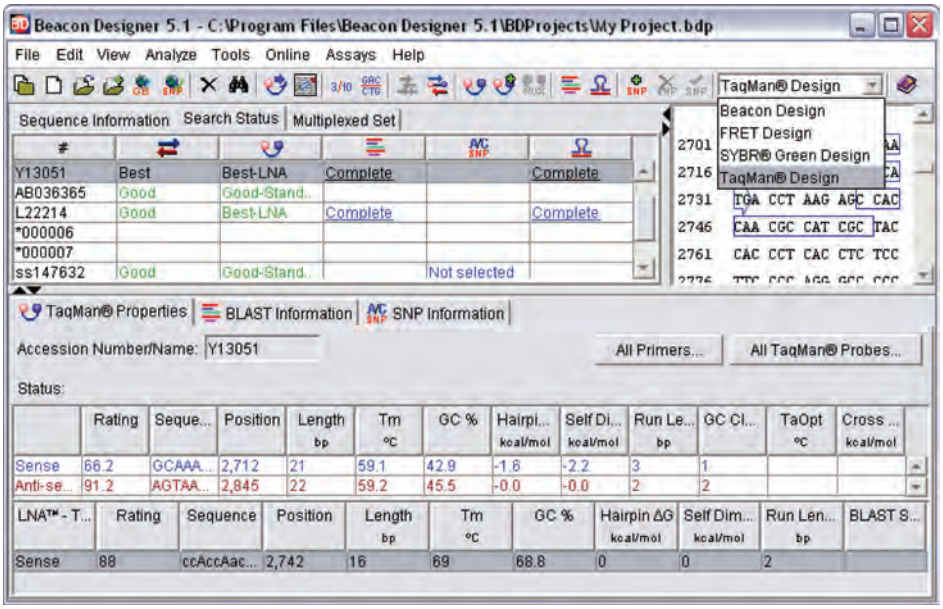

Fig. 2. A Beacon Designer project window.

Rating Feature

Beacon Designer software's search algorithm calculates a number of properties for every possible primer and probe within the specified sequence, then rates each oligonucleotide on how well it meets the search parameters. The rating is based on the T_m, calculated using the nearest-neighbor thermodynamic theory Santa Lucia values; the stability of possible secondary structures, such as self-dimer and hairpins; the location of each primer compared with the specified site; and all individual tolerances. This rating identifies the optimal primers and probes for your target sequence.

Beacon Designer 5.10 software provides fast and easy single- or multiplex primer and probe designs. The software, combined with a real-time system and PCR reagents from Bio-Rad, creates a complete system for superior real-time PCR results. A free demo version of Beacon Designer software can be downloaded from **www.premierbiosoft.com**

Beacon Designer is available from Bio-Rad if you purchase any of our real-time systems.

Ordering Information

Catalog #	Description
170-8734	Beacon Designer Probe/Primer Design Software, includes CD-ROM, quick guide, instructions
CFB-3120	MiniOpticon™ Real-Time PCR System, includes optical housing, MJ Mini™ thermal cycler, analysis software
170-9770	MyiQ™ Single-Color Real-Time PCR Detection System, includes iCycler® base, optics module, software CD-ROM, 96-well optical reaction module, optical-quality 96-well PCR plates, Microseal® 'B' seals, communication cables, power cords, instructions
CFB-3260G	Chromo4™ Four-Color Real-Time PCR System, includes optical housing, photonics shuttle, DNA Engine® thermal cycler, 96-well sample block, analysis software
170-9780	iQ™5 Multicolor Real-Time PCR Detection System, includes iCycler base, optics module, software CD-ROM, 5 installed filter sets, 96-well reaction module, calibration solutions, optical-quality 96-well PCR plates, Microseal 'B' seals, communication cables, power cord, quick reference cards, instructions

Bio-Plex™ Phosphoprotein and Total Target Assays

38 Assays to Expand Your Signal Transduction Options

Ten assays have been added to the growing list of Bio-Plex phosphoprotein and total target assays. The new release includes six phosphoprotein assays (phospho-CREB, histone H3, IRS-1, MEK1, PDGF receptor-β, and STAT6) and four total target assays (total CREB, ERK1/2, HSP27, and MEK1). These easy-to-use bead-based multiplex assays (based on xMAP technology) feature antibodies exclusively developed by Cell Signaling Technology, Inc. They are available individually or as x-Plex™ assays, which are specially premixed and quality-tested at Bio-Rad. The newest assays are listed below.

For more information, and for a complete list of assays, request bulletin 3071 or visit us on the Web at **www.bio-rad.com/products/phosphoproteins/**

Ordering Information

Catalog #	Description
Phosphoprotein Assays	
171-V26119	Bio-Plex Phospho-CREB (Ser^{133}) Assay, 1 x 96-well
171-V24777*	Bio-Plex Phospho-Histone H3 (Ser^{10}) Assay, 1 x 96-well
171-V25576	Bio-Plex Phospho-IRS-1 (Ser^{636}/Ser^{639}) Assay, 1 x 96-well
171-V25340	Bio-Plex Phospho-MEK1 (Ser^{217}/Ser^{221}) Assay, 1 x 96-well
171-V25957*	Bio-Plex Phospho-PDGF Receptor-β (Tyr^{751}) Assay, 1 x 96-well
171-V25772*	Bio-Plex Phospho-STAT6 (Tyr^{641}) Assay, 1 x 96-well
Total Target Assays	
171-V36119	Bio-Plex Total CREB Assay, 1 x 96-well
171-V32238	Bio-Plex Total ERK1/2 Assay, 1 x 96-well
171-V34551	Bio-Plex Total HSP27 Assay, 1 x 96-well
171-V35340	Bio-Plex Total MEK1 Assay, 1 x 96-well

* Refer to the matrix in bulletin 3071 or on our web site for multiplexing capabilities of specific assay combinations.

Cell Signaling TECHNOLOGY ANTIBODIES

iDQuest™ Proteome Curation Software

Manage proteomics laboratory data produced by mass spectrometric analysis of 2-D gel and liquid chromatography samples faster and more easily. iDQuest proteome curation software is a Web-based software application that manages proteomics data in a mass spectrometry laboratory environment. It is ideal for the core facility environment where vast amounts of data from different laboratories are collected.

iDQuest proteome curation software:

- Is a modular application that includes a unique curation engine to allow customization of workflow and instrument integration for your laboratory
- Gives multiple users the ability to view and run analyses on experiments wherever Internet access is available — eliminating the need for core laboratory personnel to send results to collaborating researchers, while protecting information from unauthorized access using Web-based authentication protocols
- Identifies and curates protein hits automatically in real time using all alternative information available (for example, unmatched fragments)
- Can attach multiple identification runs of multiple hits (using either different databases or different search parameters) to the data acquisition record
- Brings geographically distant researchers, instruments, and data analysis together in the context of a core workflow — data are organized hierarchically into plates, samples, experiments, and projects
- Saves data from multiple instruments to a relational database; stored results can be accessed easily using an open database connectivity (ODBC) connection; results can be compared and analyzed by searching based on experiment, sample, protein accession, protein description, and other indexed fields

iDQuest software has an intuitive, easy-to-use interface that resembles a desktop personal assistant. It integrates seamlessly with Bio-Rad's PDQuest™ and Proteomweaver™ 2-D analysis software and can be customized to work with other 2-D analysis software packages. Modules are easy to install and maintain on a standard dual CPU/core computer with 2 GB of RAM and an 80 GB hard drive. iDQuest software can support up to 50 simultaneous users.

For more information, go to **www.bio-rad.com/software/**

Ordering Information

Catalog #	Description
165-9800	iDQuest Proteome Curation Software Version 1, limit 5 users log-in
165-9850	iDQuest Software Add-On Module for Expanded Log-In Capacity, up to 50 users
165-9811	iDQuest Software Add-On Module for Integration With ABI MALDI 4700/4800 Instrument
165-9812	iDQuest Software Add-On Module for Integration With Bruker MALDI ultraflex II Instrument
165-9823	iDQuest Software Add-On Module for Integration With Finnigan LC/MS Instrument

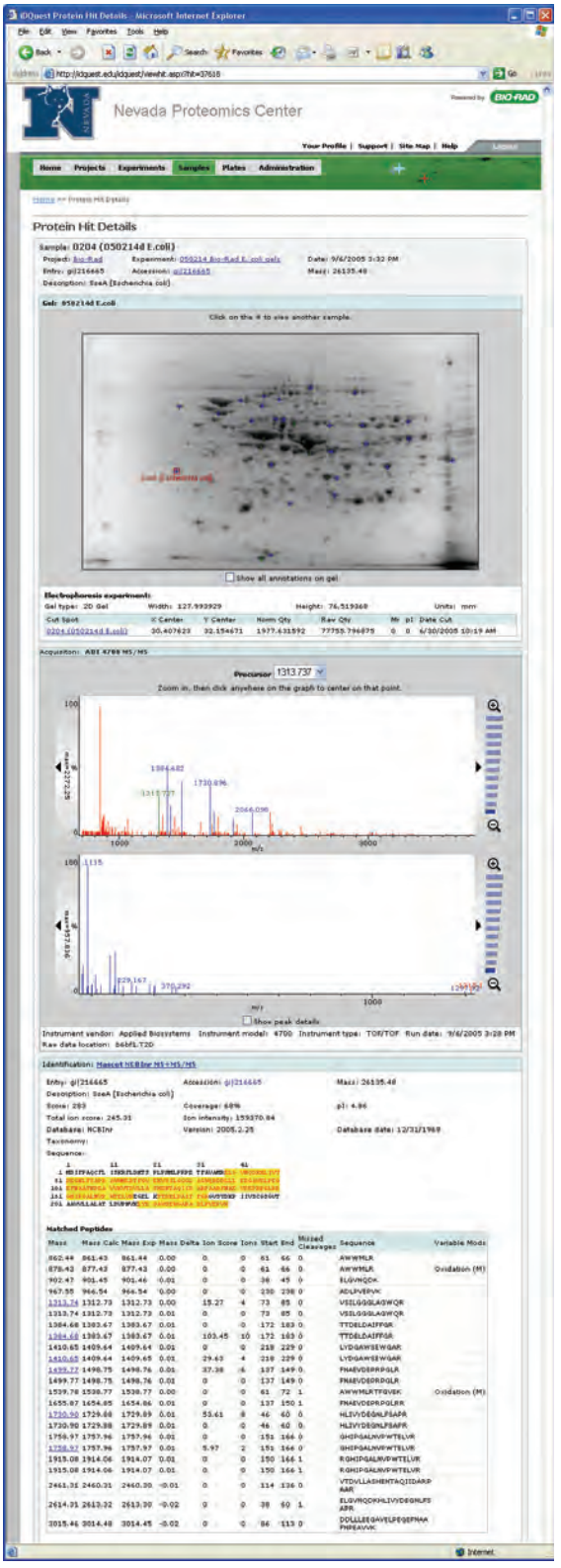

The iDQuest Protein Hit Details page. This page provides detailed information about the protein sample, including a gel image, mass spectra, protein sequences, and curated protein hits. (Courtesy of Nevada Proteomics Center, Univ of Nevada, Reno.)

Bio-Scale™ Mini Cartridges

Ready-to-Use Cartridges Include Profinity™ IMAC and UNOsphere™ Media

Bio-Scale Mini cartridges provide high-performance media in a convenient format for a wide range of chromatography applications. The quick-connect luer lock fittings adapt to any low- or medium-pressure chromatography system. Available media are:

- Profinity IMAC — provides high-purity separations of histidine-tagged proteins
- UNOsphere Q and S — strong ion exchangers that deliver high binding capacity

Additional media types will be available later in 2006 and 2007.

Ordering Information

Description	5 x 1 ml	1 x 5 ml	5 x 5 ml
Prepacked Bio-Scale Mini Cartridges			
Profinity IMAC	732-4610	732-4612	732-4614
UNOsphere Q Support	732-4100	732-4102	732-4104
UNOsphere S Support	732-4110	732-4112	732-4114

Experion™ System Software Version 2.0

Experion system software version 2.0 provides several new capabilities.

- The ability to use a user-defined internal standard for more accurate quantitation
- The ability to operate two Experion stations with one computer (when not in security mode)
- The ability to compare runs from multiple chips

Chip Compare Is Here

You can now select individual runs from multiple chips to create your own virtual chip to compare runs side by side.

Begin by selecting **New Compare Run…** from the **Analysis** menu.

Enter a name for the comparison and select the project in which you'll store the view. Choose the assay type, and then click **Next**.

All stored runs of the chosen assay type will be displayed. Select runs from the left-hand column, and click **>** to add them to the virtual chip. Remove runs from the chip by clicking **<**. Finally, choose a ladder to use for the new chip; select **Realign Data** for the best results.

Click **OK** when you are finished, and the new virtual chip will display all your information for comparison. You can save, edit, and overlay data just as you can with any other chip. The virtual chip can contain up to 40 samples.

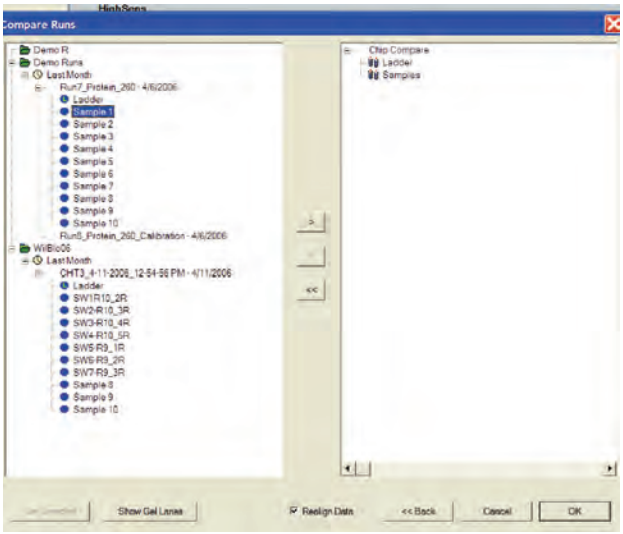

Create a custom chip for convenient comparison. The ladder lane serves as the ladder for all samples on the new chip.

For a free upgrade, contact your local Bio-Rad office for technical support.

How CHT™ Ceramic Hydroxyapatite Works

Paul Ng, Jie He, and Andrew Cohen, Bio-Rad Laboratories, Inc., Hercules, CA 94547 USA

CHT ceramic hydroxyapatite is a versatile chromatography support used for separation of biological molecules as diverse as polyclonal and monoclonal antibodies, antibody fragments, enzymes, nucleic acids, and membrane proteins. The interactions that occur between CHT and the molecules it binds are complex; this article aims to clarify the most significant features of these interactions.

CHT, $Ca_{10}(PO_4)_6(OH)_2$, is a mixed-mode support with functional groups consisting of pairs of positively charged crystal calcium ions (C-sites) and clusters of six negatively charged oxygen atoms associated with triplets of crystal phosphates (P-sites) (Figure 1). The C-sites, P-sites, and hydroxyl groups are distributed in a fixed pattern on the CHT crystal structure, as presented in classic studies by Kawasaki (1978a, 1978b) and Kawasaki et al. (1985).

In theory, CHT can retain solutes by weak anion exchange or calcium metal affinity with C-sites, by cation exchange with P-sites, and by hydrogen bonding with hydroxyl groups (Gorbunoff 1984a, 1984b, Gorbunoff and Timasheff 1984). Experimental evidence, however, suggests that most proteins bind CHT by a combination of metal affinity and phosphoryl cation exchange (Figure 2), with little contribution by hydrogen bonding. The affinity interaction of protein carboxyl clusters with CHT C-sites represents a classic metal chelating mechanism in which protein carboxyl groups approximate the carboxyl configuration of chelating agents such as EDTA. Stronger than electrostatic interactions, these metal affinity interactions withstand the presence of even saturated sodium chloride since chloride ions do not form a complex with Ca^{2+}. This indicates that any anion exchange between CHT C-sites and protein carboxyl groups does not contribute significantly to protein binding (Gorbunoff 1984a, 1984b, Gorbunoff and Timasheff 1984, Gagnon 1998). Further evidence of this comes from the demonstration that acidic proteins are retained more weakly with

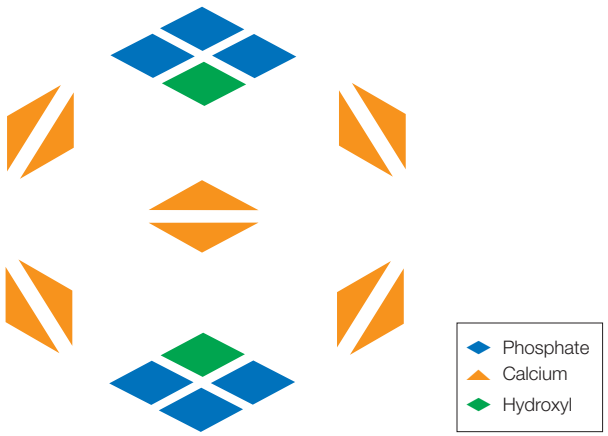

Fig. 1. Crystal structure of CHT ceramic hydroxyapatite, $Ca_{10}(PO_4)_6(OH)_2$. Each molecule consists of five positively charged calcium pairs (C-sites); two phosphate triplets (P-sites), each with six negatively charged oxygen atoms; and two hydroxyl residues.

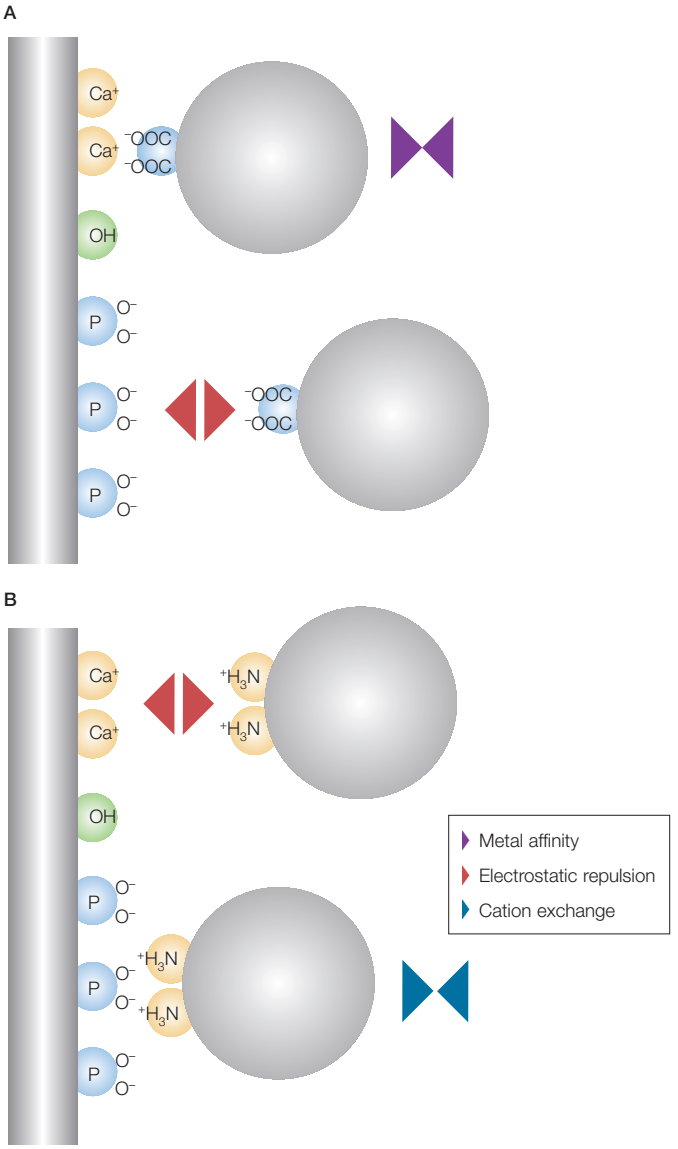

Fig. 2. Interaction of proteins with CHT. A, interaction of carboxyl groups and CHT. Note the metal affinity interaction between CHT C-sites and carboxyl groups, and the repulsion of carboxyl groups from P-sites. **B**, interaction of amino groups with CHT. Note the phosphoryl cation exchange interaction between CHT P-sites and amino groups, and the repulsion of amino groups from C-sites.

ascending pH (Ogawa and Hiraide 1995). In addition, binding experiments with urea, which disrupts hydrogen bonds (Tanford 1968, Timasheff and Fasman 1969), indicate that the contribution of hydrogen bonding is likewise negligible.

The contributions of metal affinity and phosphoryl cation exchange are distinctive for every protein and can be investigated by eluting with various neutral salt and phosphate concentrations. Elution of proteins bound by metal affinity interactions requires phosphate, which outcompetes CHT-protein metal interactions with its own strong affinity for calcium. In contrast, elution of proteins bound by cation exchange requires either neutral salts, such as sodium chloride, or buffering salts, such as phosphates. Therefore, elution of proteins by phosphate-mediated buffer can result in distinct separation, depending upon the mechanism by which the protein is bound.

Some proteins, such as lysozyme, bind CHT exclusively by cation exchange between their amino groups and CHT P-sites (Figure 2B), while others, such as bovine serum albumin (BSA), bind almost exclusively by metal affinity interactions (Figure 2A). Rich in carboxyl groups and with a strong affinity for CHT C-sites, BSA elutes in a linear phosphate gradient at pH 6.5 in 110 mM sodium phosphate (Gagnon 1998). However, when the same linear phosphate gradient is run in the presence of 1.0 M sodium chloride, the phosphate concentration required for elution of BSA drops only to 100 mM (Gagnon et al. 2005a), indicating that ion exchange is a minor contributor to the binding energy while calcium affinity dominates retention.

Still other proteins bind CHT by a combination of interaction mechanisms. Monoclonal antibodies (IgG) elute in 100–200 mM sodium phosphate (Josic et al. 1991, Bukovsky and Kennett 1987, Brooks and Stevens 1985), and unlike with BSA, even modest levels of sodium chloride sharply reduce the retention times and dynamic capacity for IgG by CHT (Gagnon 1998). This demonstrates that phosphoryl cation exchange is a major contributor to IgG binding. However, metal affinity is also a factor, albeit less so than with BSA. Though as little as 5 mM phosphate weakens binding to the point where sodium chloride can elute IgG, even this relatively weak calcium affinity must be overcome to

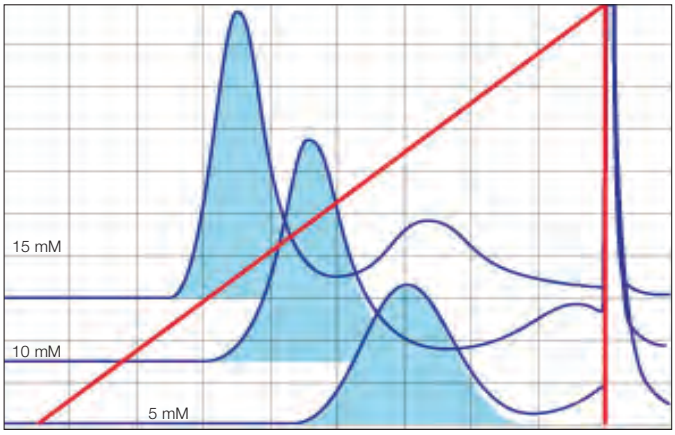

Fig. 3. Elution of protein A-purified IgG_1 from CHT ceramic hydroxyapatite. A 40 column volume linear gradient to 1.0 M NaCl (—) at three constant phosphate concentrations is shown. Data indicate a trend of decreasing aggregate resolution with increasing phosphate concentration.

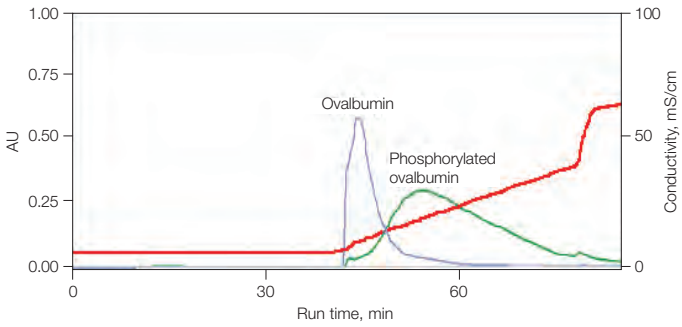

Fig. 4. Resolution of ovalbumin from its phosphorylated counterpart using CHT ceramic hydroxyapatite. Note the longer retention time for phosphorylated ovalbumin. Increasing the phosphate content of ovalbumin by conjugation of phosphoserine enhanced retention on CHT. Red trace shows conductivity (phosphate gradient).

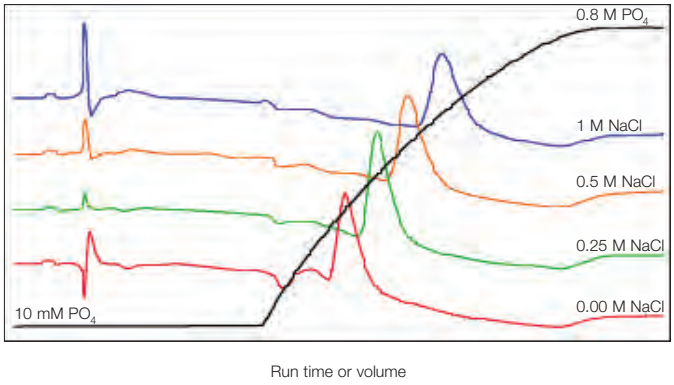

Fig. 5. Elution of sheared salmon sperm DNA from CHT ceramic hydroxyapatite. Data compare the behavior of DNA on CHT as a function of sodium chloride concentration. Increased NaCl concentration improved DNA retention.

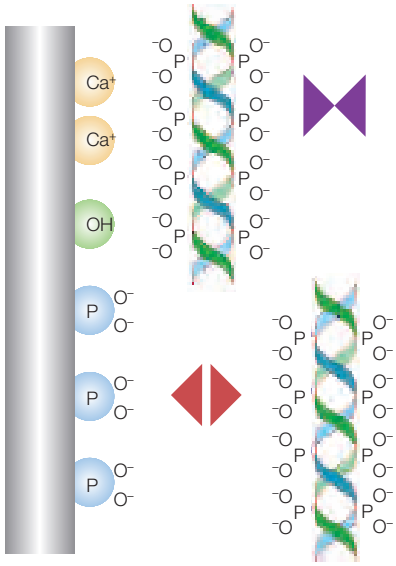

Fig. 6. Interaction of DNA with CHT ceramic hydroxyapatite. Note the electrostatic repulsion between CHT P-sites and the phosphate backbone of DNA, and the interaction of that backbone with the C-sites and hydroxyl groups. (Symbols same as in Figure 2.)

achieve elution. Unless a threshold concentration of phosphate is present, most IgGs remain bound to CHT even in saturated sodium chloride. As shown in Figure 3, retention on CHT is progressively reduced with increased phosphate concentration.

The ability of phosphate to effect elution implies that phosphorylated solutes bind strongly to CHT. In fact, phosphoryl groups on proteins and other solutes interact even more strongly with C-sites than do carboxyls (Kawasaki 1991), and phosphoproteins bind more strongly than their unphosphorylated counterparts (Ng et al. 2005a) (Figure 4). DNA, which is highly phosphorylated, binds strongly and with an apparent correlation between its size and retention time: Small fragments elute at about 0.1 M phosphate, and chromosomal DNA at 0.2–0.3 M phosphate (Kawasaki 1991, Ng et al. 2005b).

Though phosphate concentrations of 0.5 M are recommended for elution of all size classes of DNA, even higher concentrations are required if sodium chloride is present (Figure 5). This has been attributed to sodium chloride-mediated suppression of the charge repulsion between the phosphate groups on DNA and those on CHT (Figure 6). The higher conductivity obtained by adding sodium chloride may also make DNA less rigid, allowing it to conform to the geometry of available CHT C-sites (Ng et al. 2005b). Endotoxins, which are also phosphorylated, may require up to 1.0 M phosphate for complete removal; subpopulations can elute over the entire range of 0–0.5 M potassium phosphate, but reductions in retention are apparent when phosphate gradient elution is carried out at high sodium chloride concentrations, indicating that binding involves a cation exchange component (Gagnon et al. 2005b).

The mechanism by which proteins interact with CHT is multifaceted. Its unique resolution property makes it a powerful tool for process developers. The ability of CHT to purify a variety of proteins — including monoclonal antibodies, which are leading licensed products or therapeutic candidates in many drug companies — strengthens its versatility. It is anticipated that CHT will enjoy increasing attention in the years to come.

For more information, request bulletin 2156.

References

Brooks T and Stevens A, Preparative HPLC purification of IgG and IgM monoclonal antibodies, Am Lab 17, 54–64 (1985)

Bukovsky J and Kennett R, Simple and rapid purification of monoclonal antibodies from cell culture supernatants and ascites fluids by hydroxylapatite chromatography on analytical and preparative scales, Hybridoma 6, 219–228 (1987)

Gagnon P, An enigma unmasked: how hydroxyapatite works and how to make it work for you, Validated Biosystems (www.validated.com) (1998)

Gagnon P et al., Platform purification of IgG with CHT ceramic hydroxyapatite, BioProcess International Asia-Pacific Conference, 7–9 November 2005, Singapore (IBC USA Conferences, Inc., www.ibclifesciences.com) (2005a)

Gagnon P et al., Retention behavior of endotoxin, DNA and Protein A on CHT ceramic hydroxyapatite and CFT ceramic fluorapatite, BioProcess International World Conference, 19–21 September 2005, Boston, MA (IBC USA Conferences, Inc., www.ibclifesciences.com) (2005b)

Gorbunoff M, The interaction of proteins with hydroxyapatite. I. Role of protein charge and structure, Anal Biochem 136, 425–432 (1984a)

Gorbunoff M, The interaction of proteins with hydroxyapatite. II. Role of acidic and basic groups, Anal Biochem 136, 433–439 (1984b)

Gorbunoff M and Timasheff S, The interaction of proteins with hydroxyapatite. III. Mechanism, Anal Biochem 136, 440–445 (1984)

Josic D et al., Purification of monoclonal antibodies by hydroxylapatite HPLC and size exclusion HPLC, Biol Chem Hoppe Seyler 372, 149–156 (1991)

Kawasaki T, Theory of chromatography of rigid molecules on hydroxyapatite columns with small loads. IV. Estimation of the adsorption energy of nucleoside polyphosphates, J Chromatogr 151, 95–112 (1978a)

Kawasaki T, Theory of chromatography on hydroxyapatite columns with small loads, J Chromatogr 157, 7–42 (1978b)

Kawasaki T, Hydroxyapatite as a liquid chromatographic packing, J Chromatogr A 544, 147–184 (1991)

Kawasaki T et al., Hydroxyapatite high-performance liquid chromatography: column performance for proteins, Eur J Biochem 152, 361–371 (1985)

Ng P et al., Application of ceramic hydroxyapatite for proteomic analysis, ISPPP 2005, 4–6 November 2005, St Petersburg, FL (Barr Enterprises, www.isppp.org) (2005a)

Ng P et al., Differential retention of DNA on ceramic hydroxyapatite and ceramic fluoroapatite, Prep 2005, 2–6 May 2005, Philadelphia, PA (Barr Enterprises, www.prepsymposium.org) (2005b)

Ogawa T and Hiraide T, Effect of pH on gradient elution of proteins on two types of Macro-Prep® ceramic hydroxyapatite, Prep '95: Industrial Separation Science Conference, 13 February 1995, East Rutherford, NJ (1995)

Tanford C, Protein denaturation, Adv Protein Chem 23, 121–282 (1968)

Timasheff S and Fasman G, Structure and stability of biological macromolecules, Marcel Dekker, New York, NY (1969)

A Method for Rapid, Large-Scale Removal of Albumin and IgG From Human Serum Using the BioLogic DuoFlow™ Chromatography System

Fang-Fang Wu, Steve Freeby, Aran Paulus, Pete Gagnon, and Roger Provost, Bio-Rad Laboratories, Inc., Hercules, CA 94547 USA

Introduction

In human serum, albumin contributes more than 60% of total protein, and immunoglobulins, predominantly IgG, contribute 10–25%. The high concentrations of both albumin and IgG obscure low-abundance serum proteins and limit the amount of total serum protein that can be resolved by two-dimensional (2-D) electrophoresis.

The use of a chromatography system for the simultaneous removal of albumin and IgG from human serum requires the use of media that specifically remove these proteins. Affi-Gel® Blue support is a crosslinked agarose bead with covalently attached Cibacron Blue F3GA dye and efficiently removes albumin from human serum. Affi-Gel protein A support is an agarose bead coupled with protein A, which is well known for its specific binding to the Fc region of IgG molecules; it yields highly purified IgG and is also used to selectively remove IgG from human serum prior to electrophoretic analysis.

To remove both albumin and IgG from a large amount of human serum in a single, rapid process, we have developed a chromatographic method using the BioLogic DuoFlow high-resolution chromatography system. Coupled with BioLogic DuoFlow software, the system automates the processing of a biological sample on more than one column. In this study, we removed albumin and IgG from 10 ml of human serum using one AVR7-3 injection valve, one SV5-4 buffer select valve, and one SVT3-2 diverter valve to link an Affi-Gel Blue and Affi-Gel protein A column in series (Figure 1). With this configuration, albumin and IgG were removed in a single automated operation, and the BioLogic DuoFlow system was extremely productive — it showed consistent performance with virtually no user intervention. As an added benefit, this method is flexible since both the Affi-Gel Blue and the Affi-Gel protein A columns can be proportionally scaled up or down to handle varying amounts of human serum.

Methods

System Components and Buffers

The BioLogic DuoFlow chromatography system was used in this study. Components were connected to the F10 workstation and controller as illustrated in Figure 1 and included two columns (details below), a UV detector, a conductivity monitor, a BioFrac™ fraction collector, an AVR7-3 injection valve, an SV5-4 buffer select valve, and an SVT3-2 flow-diversion valve. All three buffers were filtered, degassed, and connected to the SV5-4 valve as follows: A1, equilibration buffer (50 mM sodium phosphate, 150 mM NaCl, pH 7.1); B1, elution buffer 1 (100 mM citric acid, pH 3.0); B2, elution buffer 2 (100 mM citric acid, 2 M guanidine, pH 3.0).

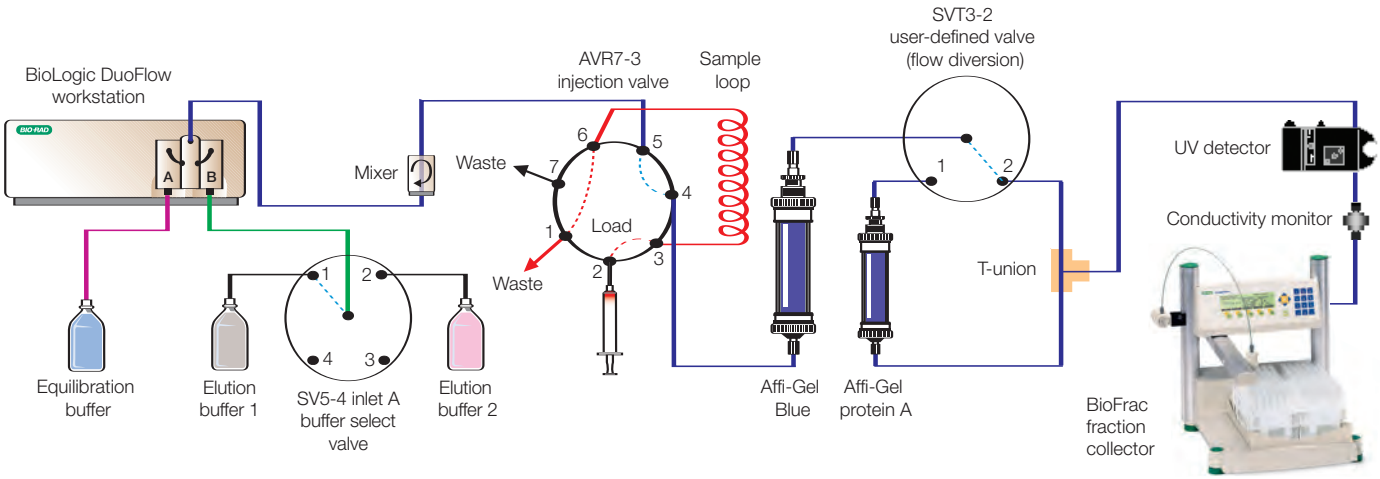

Fig. 1. Plumbing diagram of the BioLogic DuoFlow system used in this study.

Purification Protocol

A 40 ml (3.3 cm x 4.7 cm) and a 10 ml (2.3 cm x 2.4 cm) column were manually packed with Affi-Gel Blue and Affi-Gel protein A media, respectively. The AVR7-3 valve was set to load position, and the SVT3-2 valve was set to position 1 (Figure 1). Both columns were then equilibrated in series with 120 ml equilibration buffer, which corresponded to 3 column volumes (CV) of the Affi-Gel Blue column, at a flow rate of 3 ml/min. Next, 10 ml human male serum (Sigma-Aldrich Corp.) was loaded on a 10 ml injection loop and injected into the Affi-Gel Blue column through the AVR7-3 valve; flowthrough from the Affi-Gel Blue column flowed directly to the Affi-Gel protein A column. Unbound low-abundance proteins were then removed by washing both columns with 320 ml (8 CV) equilibration buffer. IgG was then eluted with 240 ml (6 CV) elution buffer 1. Once IgG was removed from the Affi-Gel protein A column, the SVT3-2 valve was switched to position 2, and albumin was eluted with 400 ml (10 CV) elution buffer 2. Following elution, the Affi-Gel Blue column was reequilibrated with 160 ml (4 CV) equilibration buffer. Then, the SVT3-2 valve was switched back to position 1, and the Affi-Gel protein A column was reequilibrated with 160 ml equilibration buffer.

In a second experiment, the 10 ml Affi-Gel protein A column was disconnected from the plumbing line and replaced with a 5 ml (1.8 cm x 2.0 cm) Affi-Gel protein A column. The same procedures described above were used except, due to the higher system pressure resulting from the narrower diameter of the smaller column, the flow rate throughout the entire procedure was decreased from 3 ml/min to 2 ml/min using the Edit All function of BioLogic DuoFlow software.

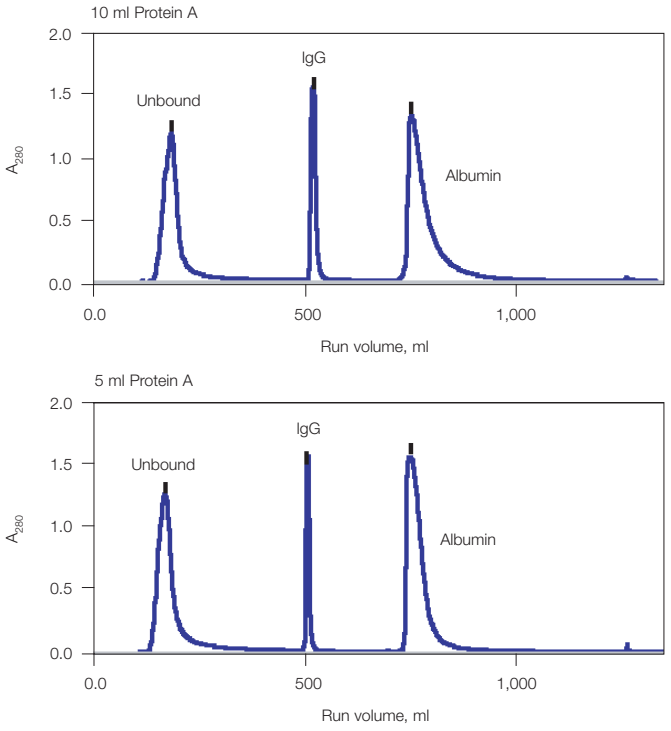

Fig. 2. Elution profiles showing removal of albumin and IgG from a human serum sample. Chromatograms plotted with BioLogic DuoFlow software are shown of separation on a 40 ml Affi-Gel Blue and a 10 ml (top panel) or 5 ml (bottom panel) Affi-Gel protein A column.

Fraction Collection and Analysis

The elution profiles from both experiments were monitored at 280 nm, and a series of 25 ml fractions was collected. To evaluate albumin and IgG removal, peak-containing fractions were analyzed by SDS-polyacrylamide gel electrophoresis (SDS-PAGE) using both reducing and nonreducing conditions and Criterion™ 4–20% gradient Tris-HCl gels. Prior to SDS-PAGE analysis, 75 µl from each fraction was desalted using a Bio-Spin® 6 Tris column. The gel resulting from separation under nonreducing conditions was analyzed using a GS-800™ densitometer and Quantity One® 1-D analysis software.

Results

A human serum sample was loaded onto a BioLogic DuoFlow chromatography system configured to use both an Affi-Gel Blue and an Affi-Gel protein A column for removal of albumin and IgG, respectively (Figure 1). Since protein A media can be costly, the relative purification efficiency achieved using different amounts of this support was also examined. The chromatograms obtained following separation on a 40 ml Affi-Gel Blue column coupled with either a 10 ml or 5 ml Affi-Gel protein A column, as plotted by BioLogic DuoFlow software, are shown in Figure 2.

SDS-PAGE analysis of the peak-containing fractions is shown in Figure 3 and indicates that both albumin and IgG were substantially removed after the human serum sample was

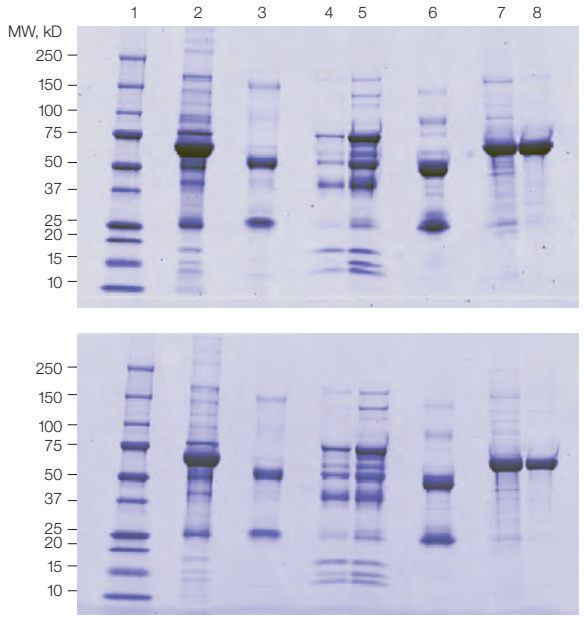

Fig. 3. SDS-PAGE analysis (reducing conditions) of fractions from Affi-Gel Blue and Affi-Gel protein A columns. Upper panel, results with 10 ml Affi-Gel protein A column; lower panel, 5 ml Affi-Gel protein A column. Both experiments were performed with a 40 ml Affi-Gel Blue column. Lane 1, Precision Plus Protein™ standards; lane 2, crude serum; lane 3, IgG standard; lanes 4 and 5, unbound proteins; lane 6, IgG elution; lanes 7 and 8, albumin elution.

subjected to processing by the Affi-Gel Blue and Affi-Gel protein A columns. For quantitation, fractions were analyzed by SDS-PAGE using nonreducing conditions, which resulted in the migration of IgG as a single band (Figure 4). Analysis of the gel in Figure 4 revealed 94% and 90% removal of albumin and IgG by the 40 ml Affi-Gel Blue and 10 ml Affi-Gel protein A columns, respectively; substitution of the 10 ml Affi-Gel protein A column with the 5 ml column resulted in 95% and 83% removal of albumin and IgG, respectively (Table 1). These results confirm that the majority of albumin and IgG was successfully removed from the human serum sample.

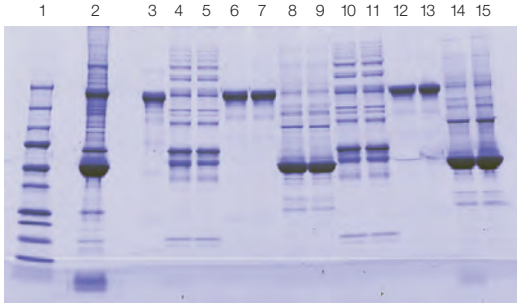

Fig. 4. SDS-PAGE analysis (nonreducing conditions) of fractions from Affi-Gel Blue and Affi-Gel protein A columns. Lane 1, marker; lane 2, crude serum; lane 3, IgG standard; lanes 4 and 5, unbound proteins from the 10 ml Affi-Gel protein A column; lanes 6 and 7, IgG elution from the 10 ml Affi-Gel protein A column; lanes 8 and 9, albumin elution from the 10 ml Affi-Gel protein A column; lanes 10 and 11, unbound proteins from the 5 ml Affi-Gel protein A column; lanes 12 and 13, IgG elution from the 5 ml Affi-Gel protein A column; lanes 14 and 15, albumin elution from the 5 ml Affi-Gel protein A column. This gel was analyzed by densitometry and Quantity One analysis software to generate the data shown in Table 1.

Table 1. Purification efficiency. Data were generated by densitometric analysis of the SDS-PAGE gel shown in Figure 4 (arbitrary units).

	Unbound	Peak	Total Volume	% Removal
40 ml Affi-Gel Blue, 10 ml Affi-Gel protein A columns				
Albumin	2.6664	39.3849	42.0513	93.66
IgG	1.2271	10.8973	12.1244	89.88
40 ml Affi-Gel Blue, 5 ml Affi-Gel protein A columns				
Albumin	2.5573	51.9654	54.5864	95.20
IgG	1.9732	9.8036	11.7890	83.16

Conclusions

The presence of high-abundance albumin and IgG in human serum masks many proteins of potential interest, especially those analyzed by 2-D electrophoresis. Affi-Gel Blue and Affi-Gel protein A media provide the high specificity and high degree of efficiency needed to meet the needs of large-scale removal of albumin and IgG from human serum. With the BioLogic DuoFlow chromatography system, separation with two media becomes a simultaneous, robust, and automated single-step process.

For additional copies of this article, request bulletin 5334.

Experion™ Automated Electrophoresis System and the Experion Pro260 Analysis Kit: Accurate and Reproducible Protein Sizing and Quantitation in the Presence of High Salt Concentrations

Karen Zhu and William Strong, Bio-Rad Laboratories, Inc., Hercules, CA 94547 USA

Introduction

Ion exchange and affinity chromatography methods are frequently used for protein separation and purification, and these methods commonly employ high concentrations of salt to effect elution of proteins from resins. Once proteins are collected, determinations of protein size (sizing) and concentration (quantitation) are carried out. Initial sizing estimates are nearly always performed using SDS-PAGE, while quantitation can be performed using gel electrophoresis, any one of a number of dye-based quantitative assays, or UV spectroscopy. The varying amounts and high concentrations of salt (generally 0.01–1.0 M) that are incorporated into many chromatographic elution buffers can be problematic for sizing and quantitation using these methods; high salt concentrations may cause band distortion or gel artifacts when the proteins are analyzed by SDS-PAGE, or they may alter background staining with protein assays, making them more variable and more cumbersome to use and necessitating careful planning and controls. Desalting prior to SDS-PAGE or a protein assay is desired in these cases, but it is sometimes not practical owing to limited sample volumes or target protein levels.

The Experion automated electrophoresis system, based on Caliper Life Sciences' LabChip microfluidic separation technology, performs rapid, reproducible, and accurate protein separation, sizing, and quantitation within a single platform. Protein analysis is performed with the Experion Pro260 analysis kit, which contains the reagents, microfluidic chips, and other supplies required for the separation and analysis of 10–260 kD proteins. Though the sizing and quantitation performance of the Experion system and Pro260 analysis kit matches or even surpasses that of SDS-PAGE (Zhu et al. 2005), this automated system must also prove reliable when the protein sample is dissolved in buffers containing high salt concentrations. Inasmuch as the Experion system relies on electrokinetic sample injection, salt concentrations can influence the amount of sample that is injected and analyzed; hence, the sensitivity of the system can be notably influenced by the ionic strength of the sample solution. In this tech note, we demonstrate the accuracy and reproducibility of protein sizing and quantitation using the Experion Pro260 analysis kit over a broad range of protein and salt (NaCl) concentrations.

Methods

Protein Samples

Purified *E. coli* β-galactosidase (116 kD), rabbit muscle phosphorylase b (97 kD), bovine liver glutamate dehydrogenase (55 kD), chicken egg ovalbumin (45 kD), rabbit muscle lactate dehydrogenase (36.5 kD), bovine milk β-lactoglobulin (18.4 kD), and chicken egg white lysozyme (14.3 kD) were purchased from Sigma-Aldrich, Inc. Bovine serum albumin (BSA, 66 kD) was purchased from the National Institute of Standards and Technology (NIST). Rabbit muscle triosephosphate isomerase (26.6 kD) was purchased from Boehringer Mannheim. Sodium chloride was purchased from VWR International, and sodium phosphate (dibasic) was purchased from EMD.

An array of 42 samples, each containing different protein and NaCl concentrations in 10 mM phosphate buffer (pH 7.2), was generated for testing. Each sample contained all nine purified proteins listed above, each at one of six concentrations (50, 100, 200, 400, 800, or 1,600 ng/µl) and one of seven NaCl concentrations (0.01, 0.05, 0.15, 0.30, 0.50, 0.75, or 1.0 M). The 0.15 M NaCl concentration, considered the optimal ionic strength for protein analysis with the Pro260 analysis kit, was used as the control.

Experion Pro260 Analysis

Experion Pro260 analysis kits include Experion Pro260 protein ladder, sample buffer, gel solution, fluorescent stain, spin filters, and microfluidic chips. Samples were prepared by mixing 2 µl Pro260 sample buffer (containing 3.2% β-mercaptoethanol) with 4 µl protein solution. Samples were heated at 95°C, diluted with 0.2 µm-filtered water, and loaded onto chips that were primed according to the protocol provided in the Pro260 analysis kit instruction manual. At least three chips (total number of wells ≥9) were run for each protein and salt combination. Statistical analysis of the sizing and quantitation data was performed using JMP software, version 5.1 (SAS Institute, Inc.). Scatter plot data representations were generated using Spotfire DecisionSite software, version 8.1 (Spotfire, Inc.).

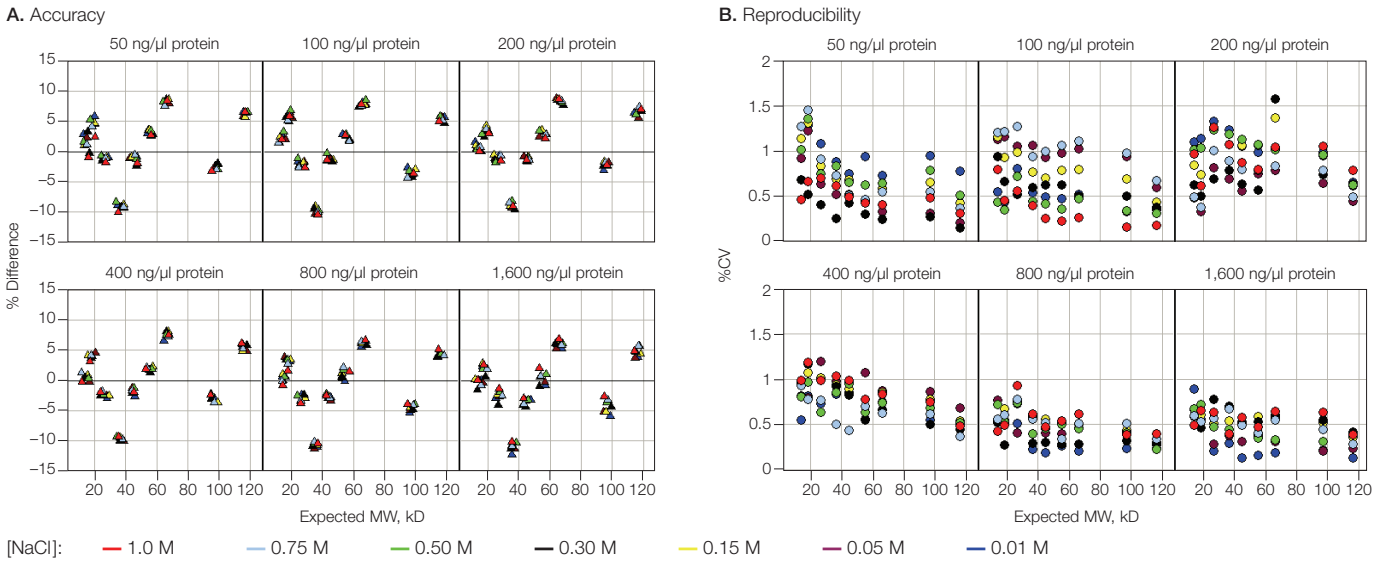

Fig. 1. Scatter plot comparisons of protein sizing accuracy (A) and reproducibility (B) for nine proteins at various concentrations and in the presence of 0.01–1.0 M NaCl. Each panel represents data for a different fixed concentration of all nine proteins, as indicated. Each colored spot represents the average of nine measurements at each experimental salt concentration (three chips with three replicate wells/chip); three chips with four replicate wells/chip were used for 0.15 M NaCl controls. Each color represents a different salt concentration.

Results and Discussion

Influence of Salt on the Accuracy and Reproducibility of Protein Sizing

Experion software automatically calculates the molecular weight (MW) for each resolved protein in a sample. To accomplish this assessment, the software first generates a calibration curve based on the migration time and known MW of each protein in the Pro260 ladder. Next, it normalizes the migration times of each sample protein by aligning each separation to the ladder lane using internal upper and lower markers that are present in each sample and that bracket the sizing range. Subsequently, the software uses the calibration curve to calculate the size of each sample protein. Sizing results are displayed in real time in an electropherogram, Results table, and simulated gel view.

To determine the impact of salt on the accuracy and reproducibility of protein sizing, we prepared and analyzed a collection of 42 samples comprised of nine proteins covering broad MW (14.3–116 kD) and concentration (50–1,600 ng/µl) ranges, and including a series of salt concentrations (0.01–1.0 M NaCl). The sizes of the nine proteins in each sample were measured, reported by Experion software, and compared to their expected MW. Accuracy, defined by the percent difference between the calculated and expected protein size, was determined using the formula: [(calculated size – expected size)/expected size] x 100. Values close to zero indicate parity between the estimated and known sizes, and a negative or positive value indicates an underestimation or overestimation, respectively. Reproducibility was evaluated using the coefficient of variation, or CV ([standard deviation/mean] x 100), as a statistical measure; CV was expressed as a percentage, with small CV values indicating a small degree of variation in replicates and good reproducibility of the quantitative data.

The data presented in each panel of Figure 1 represent the average interchip (across multiple chips) accuracy and reproducibility of protein sizing. In Figure 1, the data are divided such that at each of the six protein concentrations (50–1,600 ng/µl), a colored triangle or circle represents the % difference (Figure 1A) or %CV (Figure 1B) of a sample protein at a particular NaCl concentration. For most conditions represented, the individual data points nearly overlap, demonstrating that regardless of the protein concentration tested, increases in salt concentration from 0.01 M to 1.0 M had minimal effect on the accuracy and reproducibility of protein sizing. Despite the presence of high salt, the sizing data generated by the Experion Pro260 analysis kit were reasonably accurate, with most proteins deviating by less than 5% from expected sizes (Figure 1A); however, certain proteins, such as lactate dehydrogenase (36.5 kD) and BSA (66 kD), exhibited greater deviations from their expected MW (–11.5% and +9.1%, respectively). The results shown in Figure 1B illustrate that the sizing estimates were also highly reproducible (CV <1.6%) for all six protein concentrations and seven salt concentrations tested.

Influence of Salt on the Accuracy and Reproducibility of Protein Quantitation

The Experion Pro260 analysis kit acquires quantitative information about a protein sample by comparing the peak area of each sample protein to that of an internal standard, the 260 kD upper marker, which is present at a known concentration in each sample. Because this internal standard is present in the protein sample throughout preparation and analysis, it is presumed that any effects on quantitation that stem from differences in sample injection or separation will be experienced equally by all the proteins comprising the sample.

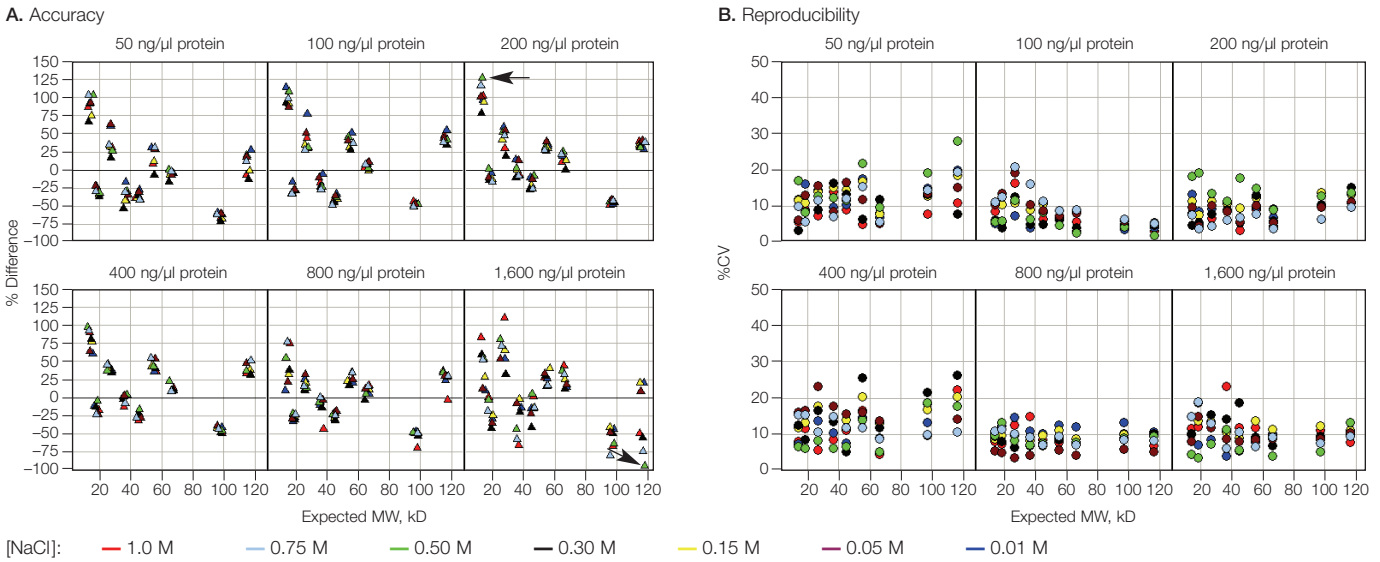

Fig. 2. Scatter plot comparison of protein quantitation accuracy (A) and reproducibility (B) for nine proteins at various concentrations and in the presence of 0.01–1.0 M NaCl. Each panel represents data for a different fixed concentration of all nine proteins, as indicated. Each colored spot represents the average of nine measurements at each experimental salt concentration (three chips with three replicate wells/chip); three chips with four replicate wells/chip were used for 0.15 M NaCl controls. Each color represents a different salt concentration, and arrows indicate maximum over- and underestimations of quantitation accuracy.

To demonstrate this concept, we compared the accuracy and reproducibility of quantitation of each protein species in the samples described previously at each of the seven NaCl concentrations (Figure 2). Depending upon the protein, deviations from expected concentrations as great as –93% (underestimate, 1,600 ng/µl β-galactosidase) to +128% (overestimate, 200 ng/µl lysozyme) were observed. Such deviations are not uncommon in other dye-based quantitation methods and are likely due to differences in the staining efficiencies of proteins (Nguyen and Strong 2005, Sapan et al. 1999). These differences indicate that certain proteins stain differently from the 260 kD upper marker since the concentration of each protein is normalized to this protein by Experion software.

Importantly, however, the level of salt in the sample appeared to have little effect on quantitation at protein concentrations up to 400 ng/µl (3.6 mg/ml total protein), as evidenced by the clustering of data points and the similar % difference values for each protein over this range of protein concentrations (Figure 2A). With protein concentrations of 800 ng/µl and greater (>7.2 mg/ml total protein), a salt-dependent effect first appeared on the quantitation accuracy of lysozyme (14.3 kD, Figure 2A), where the % difference value dramatically changed at many of the salt concentrations, as well as for the 36.5, 97, and 116 kD proteins at the 1.0 M salt concentration (red triangles). This effect on quantitation accuracy appeared to extend to the other proteins in the mix when each of their concentrations was 1,600 ng/µl (14.4 mg/ml total protein). There was no clear correlation in the data supporting the idea that the salt concentration in the sample alone reduced quantitation accuracy; rather, decreased accuracy appeared to be related to the solubility of the proteins when combined at elevated salt and total protein concentrations. In fact, several of the proteins were susceptible to precipitation at this high total protein load and at the higher salt concentrations (>0.50 M); during sample preparation, insoluble matter was visible at these protein and NaCl concentrations.

When the reproducibility of quantitation was examined, the CV for most proteins at the various protein and salt concentrations tested was generally ≤20% (Figure 2B).

Influence of Salt on Sensitivity

The results above show that by using the upper marker as an internal standard, the effect of differences in sample composition on injection and separation can be controlled, so they normally will not affect Pro260 sizing and quantitation performance. However, elevated salt concentrations can cause changes to assay sensitivity due to less sample being injected into the separation channel, resulting in visually perceptible changes in the electropherogram and gel views (Figure 3).

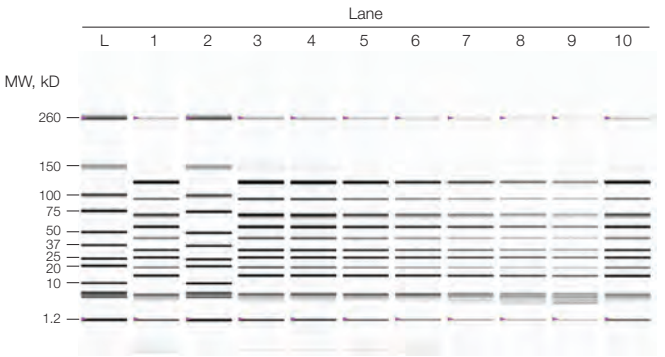

Fig. 3. Simulated gel view showing the influence of salt on detection sensitivity. Lanes L and 2, separation of Pro260 ladder; lanes 1 and 10, separation of a mixture of nine proteins in 0.15 M NaCl; lanes 3–9, separation of a mixture of nine proteins (each at 400 ng/µl) in 0.01, 0.05, 0.15, 0.30, 0.50, 0.75, and 1.0 M NaCl, respectively. Note the decreasing signal intensity at higher salt concentrations. To observe the salt-dependent effect on signal intensity, Experion software scaling was set to "Global".

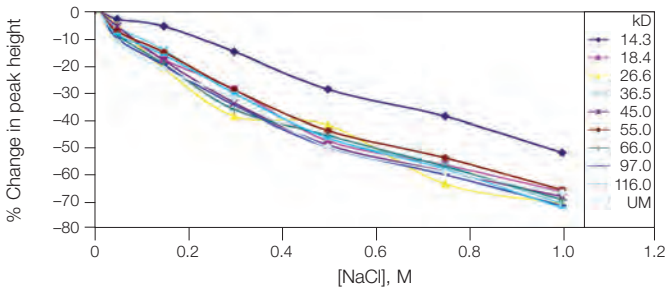

Fig. 4. Influence of salt concentration on peak height of proteins separated by the Experion system. Percentage change in peak height of each of nine proteins is plotted as a function of NaCl concentration to illustrate the dramatic decrease in peak height that occurred in buffers of increasing salt concentration. For each protein, the peak height in 0.01 M NaCl served as the reference. UM = upper marker.

To better quantitate the degree to which high ionic strength solutions affect the peak heights of proteins, we plotted the percentage change to the peak heights for each of the nine proteins in the 800 ng/µl samples. Figure 4 illustrates the plot for each of the nine proteins and shows a reduction in peak height of 5–10% for every 0.1 M increase in salt concentration. As expected, similar decreases in signal were obtained when other commonly used salts, such as KCl and $(NH_4)_2SO_4$, were tested at concentrations up to 1.0 M (data not shown). Consequently, when assessing samples in buffers containing elevated salt levels, and in cases where high sensitivity is needed (for example, when evaluating sample purity), higher protein concentrations may be required to compensate for reduced peak heights.

Conclusions

When protein samples are analyzed using the Experion automated electrophoresis system and the Experion Pro260 analysis kit, the presence of high salt (up to 1.0 M NaCl) in the sample does not appear to significantly alter the accuracy and reproducibility of sizing and quantitation, even though there is a notable decline in signal strength as salt levels are increased. This result applied equally to every one of nine different proteins, where the amount of each protein spanned a concentration range of 50–400 ng/µl, for a total protein load of 0.45–3.6 mg/ml. However, these quantitation parameters may vary at lower protein concentrations (<50 ng/µl) and when the salt concentration or ionic strength of the sample solution is elevated (>1.0 M), because the peak heights for all proteins decrease under these conditions and lead to lower overall assay sensitivity. Additionally, a combination of high protein (>800 ng/µl) and high salt concentrations (>0.50 M NaCl) can lead to protein precipitation, which may influence the level of protein in a sample, thereby affecting quantitation accuracy.

References

Nguyen M and Strong W, Performance comparison of the Experion automated electrophoresis system and a competing automated system for protein analysis, Bio-Rad bulletin 5302 (2005)

Sapan CV et al., Colorimetric protein assay techniques, Biotechnol Appl Biochem 29, 99–108 (1999)

Zhu K et al., Performance comparison of the Experion automated electrophoresis system and SDS-PAGE for protein analysis, Bio-Rad bulletin 5299 (2005)

For additional copies of this article, request bulletin 5328.

www.bio-rad.com/RNAi/

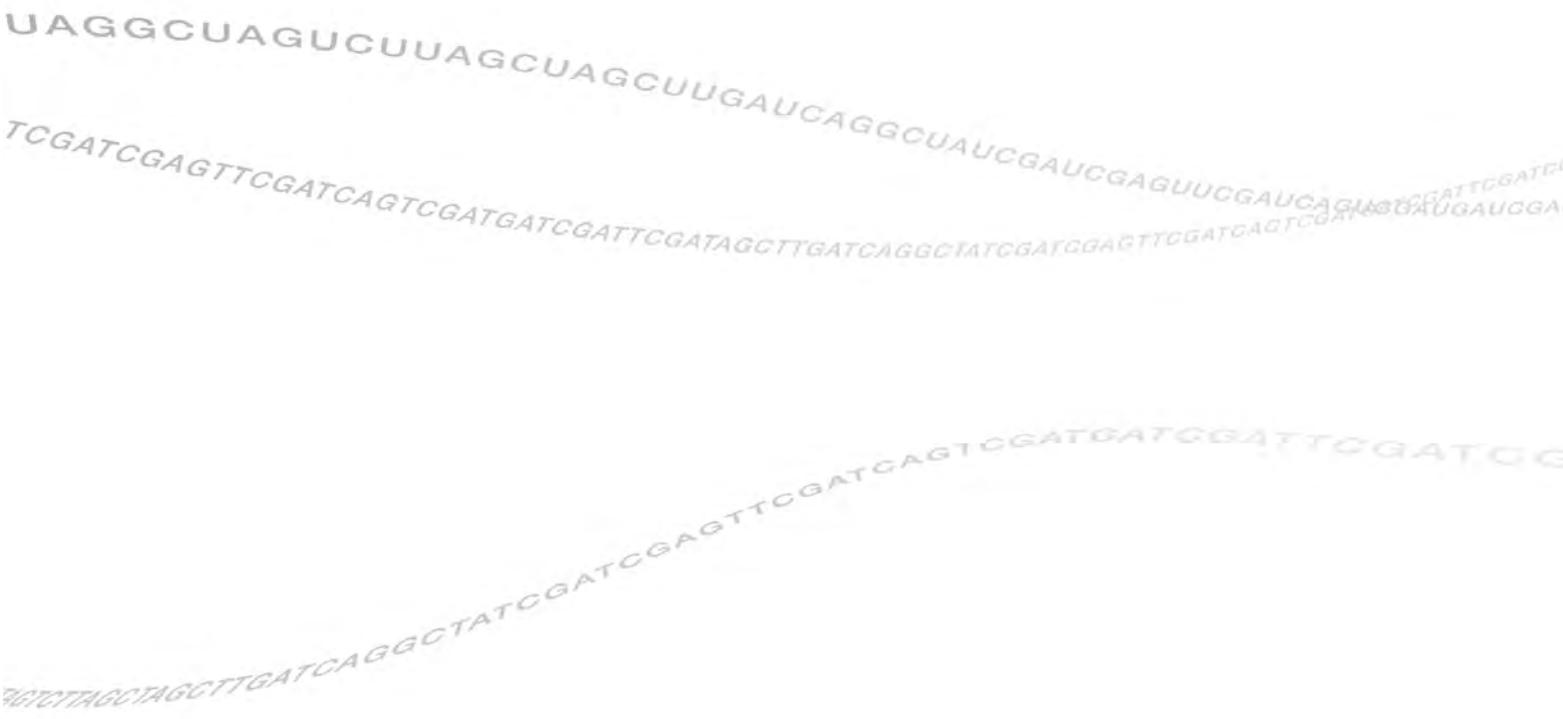

Dicer-Substrate siRNA Technology

Advances in siRNA Designs Improve Gene-Specific Silencing

Steve Kulisch, Teresa Esch, Christina Whitman-Guliaev, and Teresa Rubio, Bio-Rad Laboratories, Inc.

RNA interference (RNAi) is an intrinsic cellular mechanism, conserved in most eukaryotes, that helps to regulate the expression of genes critical to cell fate determination, differentiation, survival, and defense from viral infection. Researchers have exploited this natural mechanism by designing synthetic double-stranded RNAs (dsRNAs) for sequence-specific gene silencing to elucidate gene function (Hannon 2002, Hutvagner and Zamore 2002, Sharp 1999). Such research has helped forge a rapid transition from discovery and research to potential therapeutic application (Xia et al. 2004).

Since it was first demonstrated that 19–23 nt small interfering RNAs (siRNAs) are mediators of gene-specific silencing (Elbashir et al. 2001a), design of siRNAs has sought to improve specificity and potency, which can reduce off-target effects (Birmingham et al. 2006, Jagla et al. 2005, Naito et al. 2004). While traditional synthetic siRNAs based on the 21- to 23-mer designs have been effective, increased understanding of the discrete events and enzymes involved in the RNAi pathway have recently led to significant improvements in the design of siRNAs, making them even more efficient tools for the induction, control, and interpretation of gene silencing events in everyday research (Khvorova et al. 2003, Schwarz et al. 2003). This article describes studies by researchers at City of Hope and Integrated DNA Technologies (IDT) that led to the development of one such tool, Dicer-substrate siRNA, a highly potent mediator of RNAi.

RNAi Overview

The RNAi pathway, part of a larger network that uses small RNA molecules as regulators of cellular signaling, relies on dsRNA as a trigger for sequence-specific gene silencing (Figure 1). In this pathway, longer dsRNAs associate with Dicer endonuclease, a member of the RNase III family, which precisely cleaves the dsRNA into smaller functional siRNAs (MacRae et al. 2006). These siRNAs then associate with an RNA-induced silencing complex (RISC), which targets any homologous mRNA for degradation. It has recently been suggested that in addition to cleaving longer dsRNAs, Dicer endonuclease plays roles in loading processed dsRNA into RISC and in RISC assembly (Lee et al. 2004, Rose et al. 2005, Sontheimer 2005). This hypothesis has helped drive the development of a new class of siRNAs, termed Dicer-substrate siRNAs, that are highly potent mediators of gene-specific silencing.

25- to 30-mers are up to 100-fold more potent than 21-mer siRNAs targeting the same sequence.

Dicer-Substrate siRNA

While long (>30 nt) dsRNAs have been used successfully to regulate gene expression in a number of eukaryotic organisms, including fungi, plants, and *C. elegans* (Napoli et al. 1990, Romano and Macino 1992, Fire et al. 1998), they often activate intrinsic cellular immune responses that result in broad, nonspecific silencing when applied to mammalian systems (Minks et al. 1979, Stark et al. 1998). To prevent activation of these immune responses during RNAi experiments, researchers have generally used shorter (19–23 nt) dsRNAs (Elbashir et al. 2001b).

More recent studies have demonstrated that dsRNAs 25–30 nt in length are even more powerful effectors of gene-specific silencing than 21-mers. Specifically, 25- to 30-mers are up to 100-fold more potent than 21-mer siRNAs targeting the same sequence (Kim et al. 2005). This greater potency appears to depend on processing of the longer dsRNAs by Dicer, which cleaves the longer dsRNAs to produce 21-mers. When 27-mer siRNAs were selectively labeled with 6-carboxyfluorescein (6-FAM) to reduce cleavage by Dicer, a corresponding decrease in potency of siRNA was observed (Kim et al. 2005).

Dicer cleavage of 27-mers into specific 21-mers does not, by itself, explain the greater potency of the 27-mers. Different 21-mer siRNAs (with 2-base 3' overhangs) were synthesized to correspond to all possible Dicer products that could be derived from a blunt 27-mer duplex. None of these 21-mers, acting individually or pooled, produced the same level of silencing observed with 27-mers at low concentrations of siRNA (Kim et al. 2005). Since specific cleavage by Dicer is not sufficient to explain the increased potency, it has been hypothesized that providing Dicer with a substrate for cleavage (i.e., a 27-mer) improves the efficiency of the secondary role of Dicer — that of introducing siRNAs into RISC — and that this is responsible for the enhanced silencing by 27-mers (Rose et al. 2005).

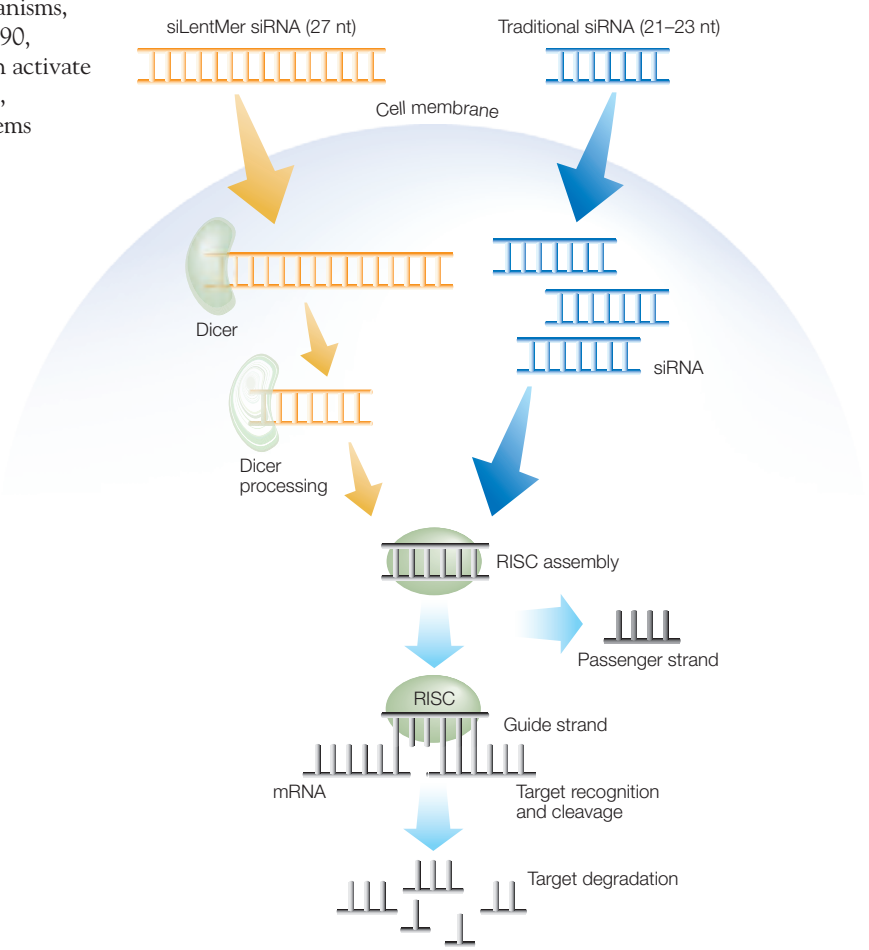

Fig. 1. Activation of the RNAi pathway by dsRNAs. Long dsRNAs are cleaved by Dicer endonuclease to form 21–23 nt duplexes. After cleavage, siRNA duplexes are incorporated into RISC. Unwinding of the siRNA duplex results in retention of the guide strand. The guide strand then pairs with complementary mRNA sequences, which are cleaved by RISC and degraded. This allows silencing of a specific gene. Dicer, in addition to cleaving dsRNAs longer than 21 nt, may facilitate the loading of siRNAs into RISC. This may explain why synthetic 21-mer dsRNAs, which are not cleaved by Dicer, are less effective than 27-mers containing the same sequence. Because Dicer may influence loading, and because siRNA structure influences the orientation of Dicer binding, Dicer-substrate siRNAs can be designed to promote specific cleavage by Dicer and preferential retention of the guide strand complementary to the target mRNA.

Asymmetric Design of 27-mers Confers Functional Polarity

Subsequent work on Dicer-substrate siRNAs has sought to improve their design to further increase the efficacy of silencing (Rose et al. 2005). General rules of siRNA duplex design, such as length, sequence preference, and target accessibility, play a role in the relative potency of any given siRNA (Reynolds et al. 2004, Brown et al. 2005, Overhoff et al. 2005). In addition to these rules, Dicer-substrate siRNAs can be designed to promote Dicer cleavage at a specific position to produce the most potent 21-mer product. Additional subtle design features can influence the dynamics of strand incorporation into RISC, promoting selective retention of the guide strand (the antisense strand, which is complementary to the target message) and leading to a significant impact on the performance of siRNAs in vitro.

Dicer-substrate siRNAs are potent at concentrations as low as 100 pM, which minimizes the potential for off-target effects.

By using electrospray ionization mass spectrometry (ESI-MS) to analyze the Dicer products derived from a variety of 27-mers, researchers at IDT and City of Hope were able to identify structural features that encourage the production of a single, predictable, maximally active product (Rose et al. 2005). Specifically, an asymmetric design that includes a 2-base 3' overhang on one strand and the addition of 2 DNA residues to the 3' end of the other strand (Figure 2) severely limits heterogeneity of the cleaved siRNA product — the blunt end is unfavorable for Dicer binding, and cleavage preferentially occurs 21–22 bases from the overhang. Maximum potency is obtained when the 2-base overhang is present on the antisense strand while the DNA bases are added to the sense strand. In this case, Dicer binds to the 5' end of the antisense strand, leading to preferential retention of this strand in RISC. These design features, which are incorporated into Bio-Rad's siLentMer Dicer-substrate siRNAs (see sidebar, next page), ensure maximum potency in RNAi.

Benefits of Dicer-Substrate siRNAs

Effective use of RNAi for research and therapeutics requires that nonspecific effects be minimized. Nonspecific effects may be related to sequence homology of an untargeted mRNA or activation of cellular responses — particularly induction of the interferon response, which can result in global translational arrest. In addition, some data suggest that the RNAi machinery can be saturated, inhibiting the proper processing of precursors of microRNA (miRNA; Bitko et al. 2005), leading to toxicity. Nonspecific effects and toxicity can be limited by using low concentrations of siRNA. For example, while full activation of the interferon pathway can be avoided by the modest use of siRNAs <30 nt in length (Elbashir et al. 2001a), proinflammatory responses can be activated by higher concentrations of siRNA (Persengiev et al. 2004). Dicer-substrate siRNAs, when used with an effective transfection reagent and protocol, are potent at concentrations as low as 100 pM (see figure in sidebar), which minimizes the potential for off-target effects. To further reduce the potential for activating immune responses, Dicer-substrate siRNAs can be specifically designed to prevent the activation of proinflammatory cytokines (IFN-α and IFN-β) and the protein kinase R (PKR) pathway (Kim et al. 2004). To demonstrate this, cells were transfected with a 27-mer dsRNA, a 21-mer siRNA, or a triphosphate-containing single-stranded RNA (ssRNA). The latter was used as a positive control, because it is highly effective in activating IFN-α and IFN-β when introduced into cells. Compared to cells transfected with ssRNA, assays of cell lysates from cells transfected with 27-mer dsRNA or 21-mer siRNA showed no detectable levels of IFN-α and IFN-β and no evidence of PKR activation. While the risk of other off-target effects remains, this risk can be tempered by using reagents that permit the use of low nanomolar concentrations of siRNA (Persengiev et al. 2004).

An additional benefit of Dicer-substrate siRNAs is longevity of silencing. When NIH 3T3 cells stably expressing enhanced Green Fluorescent Protein (eGFP) were transfected with 21-mers or 27-mers targeting the same site, eGFP suppression by the 21-mer lasted for about 4 days, while suppression by the 27-mer lasted up to 10 days (Kim et al. 2005). While these results match observations made in other studies (Persengiev et al. 2004), some 21-mer siRNAs, described as hyperfunctional siRNAs, can produce comparable long-term silencing (Reynolds et al. 2004). Still, controlling the processing of 27-mers by Dicer to ensure the production of a single specific siRNA can allow lasting and consistently potent silencing at low concentrations and reduce the chance of off-target silencing events.

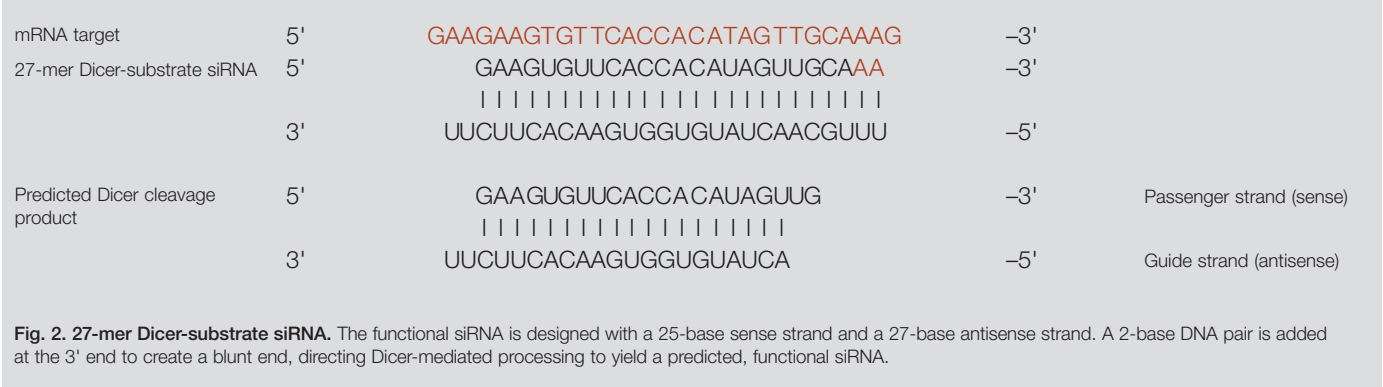

Fig. 2. 27-mer Dicer-substrate siRNA. The functional siRNA is designed with a 25-base sense strand and a 27-base antisense strand. A 2-base DNA pair is added at the 3' end to create a blunt end, directing Dicer-mediated processing to yield a predicted, functional siRNA.

Summary

Synthetic 27-mer Dicer-substrate dsRNAs can be designed to be processed by Dicer in a predictable way, to ensure appropriately oriented loading into RISC and thus maximum efficiency in RNAi. Use of an efficient transfection method allows these siRNAs to be used at low concentrations, minimizing the potential for off-target effects.

References

Birmingham A et al., 3' UTR seed matches, but not overall identity, are associated with RNAi off-targets, Nat Methods 3, 199–204 (2006)

Bitko V et al., Inhibition of respiratory viruses by nasally administered siRNA, Nat Med 11, 50–55 (2005)

Brown KM et al., Target accessibility dictates the potency of human RISC, Nat Struct Mol Biol 12, 469–470 (2005)

Elbashir SM et al., RNA interference is mediated by 21- and 22-nucleotide RNAs, Genes Dev 15, 188–200 (2001a)

Elbashir SM et al., Duplexes of 21-nucleotide RNAs mediate RNA interference in cultured mammalian cells, Nature 411, 494–498 (2001b)

Fire A et al., Potent and specific genetic interference by double-stranded RNA in *Caenorhabditis elegans*, Nature 391, 806–811 (1998)

Hannon GJ, RNA interference, Nature 418, 244–251 (2002)

Hutvagner G and Zamore PD, RNAi: nature abhors a double-strand, Curr Opin Genet Dev 12, 225–232 (2002)

Jagla B et al., Sequence characteristics of functional siRNAs, RNA 11, 864–872 (2005)

Khvorova A et al., Functional siRNAs and miRNAs exhibit strand bias, Cell 115, 209–216 (2003)

Kim DH et al., Interferon induction by siRNAs and ssRNAs synthesized by phage polymerase, Nat Biotechnol 22, 321–325 (2004)

Kim DH et al., Synthetic dsRNA Dicer substrates enhance RNAi potency and efficacy, Nat Biotechnol 23, 222–226 (2005)

Lee YS et al., Distinct roles for *Drosophila* Dicer-1 and Dicer-2 in the siRNA/miRNA silencing pathways, Cell 117, 69–81 (2004)

MacRae IJ et al., Structural basis for double-stranded RNA processing by Dicer, Science 311, 195–198 (2006)

Minks MA et al., Synthesis of 2'5'-oligo(A) in extracts of interferon-treated HeLa cells, J Biol Chem 254, 5058–5064 (1979)

Naito Y et al., siDirect: highly effective, target-specific siRNA design software for mammalian RNA interference, Nucleic Acids Res 32, W124–W129 (2004)

Napoli C et al., Introduction of a chimeric chalcone synthase gene into petunia results in reversible co-suppression of homologous genes in trans, Plant Cell 2, 279–289 (1990)

Overhoff M et al., Local RNA target structure influences siRNA efficacy: a systematic global analysis, J Mol Biol 348, 871–881 (2005)

Persengiev SP et al., Nonspecific, concentration-dependent stimulation and repression of mammalian gene expression by small interfering RNAs (siRNAs), RNA 10, 12–18 (2004)

Reynolds A et al., Rational siRNA design for RNA interference, Nat Biotechnol 22, 326–330 (2004)

Romano N and Macino G, Quelling: transient inactivation of gene expression in *Neurospora crassa* by transformation with homologous sequences, Mol Microbiol 6, 3343–3353 (1992)

Rose SD et al., Functional polarity is introduced by Dicer processing of short substrate RNAs, Nucleic Acids Res 33, 4140–4156 (2005)

Schwarz DS et al., Asymmetry in the assembly of the RNAi enzyme complex, Cell 115, 199–208 (2003)

Sharp PA, RNAi and double-strand RNA, Genes Dev 13, 139–141 (1999)

Sontheimer EJ, Assembly and function of RNA silencing complexes, Nat Rev Mol Cell Biol 6, 127–138 (2005)

Stark GR et al., How cells respond to interferons, Annu Rev Biochem 67, 227–264 (1998)

Xia H et al., RNAi suppresses polyglutamine-induced neurodegeneration in a model of spinocerebellar ataxia, Nat Med 10, 816–820 (2004)

Bio-Rad Partners With Integrated DNA Technologies (IDT) to Provide siLentMer Products

Bio-Rad Laboratories offers a selection of 27-mer Dicer-substrate siRNAs, including siRNAs validated to achieve ≥85% knockdown of mRNA in specific human genes. Bio-Rad has combined its effective transfection and analysis capabilities with IDT's expertise in high-quality oligonucleotide manufacturing and quality control to produce these siLentMer 27-mer Dicer-substrate siRNAs. The siRNAs are designed using an advanced algorithm that incorporates the design features discussed in the accompanying article. Final siRNA designs undergo a comprehensive bioinformatic analysis to avoid homology to other sequences and to ensure specific targeting. Any siRNAs targeting alternatively spliced exons or known single nucleotide polymorphisms (SNPs) are eliminated. siLentMer siRNAs are effective at low concentrations (as low as 100 pM), and this helps minimize the potential for off-target silencing that is typically associated with siRNAs that are effective only at higher concentrations.

siLentMer Dicer-Substrate siRNA Duplexes

Validated and predesigned siLentMer siRNAs offer convenience by saving the time and expense of developing and screening your own effective siRNA libraries. Multiple siRNA duplexes are available for a variety of targets. This allows you to confirm knockdown results in a specific gene of interest by duplicating the biological effects using additional siRNAs. Both validated and predesigned siLentMer Dicer-substrate siRNA duplexes are purified by HPLC and identified by ESI-MS.

Validated siRNAs

- Functionally tested by RT-qPCR to guarantee a reduction in mRNA levels by ≥85%
- Validated at siRNA concentrations as low as 5 nM to reduce the chance of off-target effects and toxicity
- Appropriate for targeting a gene of interest or as an experimental control
- Available with up to 2 different siRNA duplexes per target to better confirm that any biological effects observed in experiments are specifically due to loss of the targeted gene

In addition to individual duplexes, selections of validated siRNA duplexes are combined with controls and siLentFect™ lipid reagent for RNAi to create transfection kits. These easy-to-use kits are ideal for optimization.

Predesigned siRNAs

- Ready-to-order duplexes for various gene targets
- Useful when a validated siRNA is not yet available
- Generally more efficient at lower concentrations (≥5 nM) than 21-mer siRNAs
- Available with up to 4 different siRNA duplexes per target to investigate effectiveness of target gene knockdown

27-mer

siLentMer siRNA Transfection Kits

When performing RNAi experiments, it is important to establish effective silencing conditions and a set of positive and negative controls for your cell line. To simplify optimization of transfection conditions, selection of appropriate controls, and assessment of the efficiency of siRNA delivery, siLentMer transfection kits combine siLentFect lipid reagent with both validated and fluorescently labeled siLentMer siRNA duplexes.

Delivery Optimization Kit

- Contains all the components for establishing optimal delivery conditions for most cell lines
- Includes a fluorescently labeled nonsilencing siRNA and siLentFect lipid reagent
- Contains sufficient reagents for approximately 150 transfections in 24-well plates

Starter Kits

- Help optimize delivery conditions and establish reliable positive and negative controls for cell lines
- Include a validated Dicer-substrate siRNA, nonsilencing negative control siRNA, and siLentFect lipid reagent
- Contain sufficient reagents for approximately 150 transfections in 24-well plates

Total Control Kits

- Contain all the appropriate positive and negative controls to optimize delivery and fully evaluate target silencing
- Include a validated Dicer-substrate siRNA, nonsilencing negative control siRNA, fluorescently labeled nonsilencing siRNA, and siLentFect lipid reagent
- Are available with GFP or luciferase validated siRNAs for cotransfection experiments involving plasmid-based reporter genes
- Contain sufficient reagents for approximately 300 transfections in 24-well plates

siLentFect — An Effective Lipid Transfection Reagent

Lipid-mediated transfection is the most popular method for siRNA delivery because it is the most affordable, simple, and consistent delivery method for performing RNAi. Furthermore, it can be broadly applied to a variety of cell lines with effective silencing results.

Bio-Rad's siLentFect lipid transfection reagent was specifically developed to deliver siRNA into cells. siLentFect reagent's high molar efficiency requires only low concentrations of siRNA and small lipid volumes to achieve silencing of up to 90%.

Custom siRNAs

Bio-Rad's siRNA partner, IDT, specializes in manufacturing custom DNA and RNA oligonucleotides for research applications. IDT has the expertise to deliver custom-synthesized RNA with the yield and purity that researchers demand. Go to **www.idtdna.com** for custom siRNA synthesis inquiries.

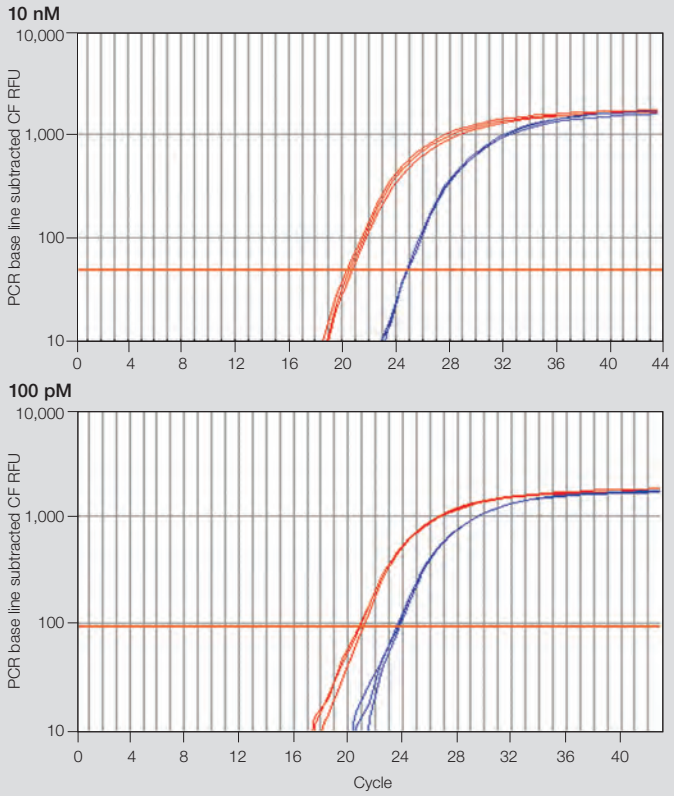

Effective silencing can be achieved with very low siRNA concentrations using siLentMer Dicer-substrate siRNAs and siLentFect lipid reagent. HeLa cells were grown in 24-well plates to ~70% confluence and transfected with 10 nM or 100 pM of siLentMer Dicer-substrate siRNAs targeting HPRT, or with an anti-EGFP control. 24 hr posttransfection, RNA was purified and RT-qPCR was performed on the iCycler iQ® system. At both concentrations, HPRT (—) was silenced >85% relative to the control (—).

Research Resources

Bio-Rad offers a variety of resources to assist you with your research. Our support groups (technical support teams, customer service, field application specialists, etc.) are knowledgeable, responsive, and available to help provide necessary information.

The new Gene Expression Gateway (GXG) web site (**www.bio-rad.com/genomics/**) is a valuable application-focused resource for genomic research and Bio-Rad products. The site provides information for the four main application areas consistent with the gene expression workflow — sample preparation, quantification, profiling, and modulation. Another key element of the GXG site is the Citations Library, a searchable database of over 10,000 published research articles citing Bio-Rad products for genomics.

Specific information on RNAi applications is available on the Bio-Rad RNAi web site (**www.bio-rad.com/RNAi/**). From design to detection, Bio-Rad offers an extensive set of tools for effective gene silencing and analysis. Potent Dicer-substrate siRNAs, three delivery technologies, and four detection platforms are supported by high-quality sample preparation kits and quality analysis tools for both RNA and protein methodologies.

www.bio-rad.com/RNAi/

Proteomic Analysis of Tumor Biomarkers in Human Clinical Specimens Using the BioOdyssey™ Calligrapher™ MiniArrayer

Nere Navarro and Phillip E Schwartz, Protein Biotechnologies, Inc., Ramona, CA 92065 USA

Introduction

Reverse-phase protein microarray (RPPA) technology is a powerful emerging analytic strategy for interrogating the proteomes of tissues and cells. As a high-throughput screening platform, RPPA permits rapid quantitative identification of novel cancer biomarkers associated with oncogenesis and disease progression. RPPA should be useful in accelerating the understanding of cellular differentiation, transformation, angiogenesis, tumorigenesis, and metastasis. This new technology has the ability to quickly elucidate alterations in protein expression levels, detect posttranslational modification and mRNA processing events, and dissect molecular networks associated with drug administration or exposure to environmental factors (for example, toxins, infectious agents, or radiation). With this new ability, cancer researchers, clinicians, and, more importantly, patients should realize a significant benefit in biomarker discovery, molecular diagnostics, drug development, and personalized medicine.

Innovations that increase the production, quality, and performance of protein microarrays are critical to realizing the full potential of this screening platform. Laboratories engaged in high-throughput protein biomarker identification and discovery require protein microarray products and methods that are easy to analyze, are easy to automate, and ensure consistent results. The amount of information obtained from current protein microarray experiments is limited to what one probe and slide can generate, and thus these experiments can consume an excessive amount of expensive resources, reagents, and clinical tissue samples. Realizing the full scientific and healthcare benefits of RPPA will require that sample throughput and sensitivity be maximized. Significant cost reductions can be achieved by using innovative multiplex detection systems to probe multiple samples with multiple analytes in a single assay.

In our laboratory, we have developed a line of ready-to-use protein microarrays for cancer research. Arrays are fabricated using lysates prepared from an extensive collection of human tumor and normal clinical specimens representing a variety of organs, tissues, and cancer subtypes. Our approach is similar to that used to evaluate protein expression in the NCI-60 cancer cell lines (Nishizuka et al. 2003) and biopsy samples in clinical trial research (Gulmann et al. 2005). We are also developing sensitive detection systems that would permit automated multiplex analysis of multiple targets in a single assay. The development and manufacturing of our products require a robust and consistent arraying platform with exceptional spot-tracking features for quality control and run validation.

Detection sensitivity is an inherent challenge in the use of protein microarrays, especially for the detection of specific proteins in complex biological samples such as cell or tissue lysates. Spot sizes are often small (~100–300 µm), and the amount of target protein available for detection is correspondingly reduced. The choice of detection methods (chromogen, chemiluminescence, fluorescence, etc.) also influences the detection limits of the assay. Finally, data capture and image analysis hardware and software vary greatly in sensitivity, flexibility, and of course cost. Therefore, to maximize the data obtained from an experiment, it is important to maximize sensitivity.

We wished to evaluate parameters affecting the use of prote in microarrays and the quality of the data obtained from experiments using them. To determine specificity and sensitivity criteria in our system, we prepared a special batch of microarray slides using lysates from lung, breast, and colon tissue. Slides were interrogated with individual antibodies specific for known biomarkers involved in oncogenesis, vascularization, the extracellular matrix, and cell maintenance. Target visualization was performed using a chromogen detection system, and microarray images were acquired and processed.

Methods

Six pairs of patient-matched normal and tumor tissue protein extracts from colon, breast, and lung were spotted in triplicate on specially prepared nitrocellulose-coated glass slides (Grace Bio-Labs, Inc.). Arrays were printed using a BioOdyssey Calligrapher miniarrayer with TeleChem Stealth SMP6 micro spotting pins, producing 160 µm spots, delivering ~2.0 nl/spot of a 1.0 mg/ml protein solution. Lysates were spotted in modified RIPA protein extraction buffer according to the manufacturer's recommended protocols. Positive (purified IgGs) and negative (buffer only and BSA) controls were also included in the arrays. Sample tracking and spot placement were validated using the BackTracker™ file system, which is built into the miniarrayer software.

Slides were treated using protocols similar to those for western blotting of proteins transferred to nitrocellulose membranes (Krajewski et al. 1996). Monoclonal and polyclonal primary antibodies raised against β-actin, tubulin (Imgenex Corp.), glyceraldehyde-3-phosphate dehydrogenase and laminin-1 (Proteus BioSciences, Inc.), human IgG, and rabbit IgG (Jackson ImmunoResearch Laboratories, Inc.) were used according to suppliers' recommendations and detected using HRP-conjugated secondary antibodies (Protein Biotechnologies, Inc.). Color

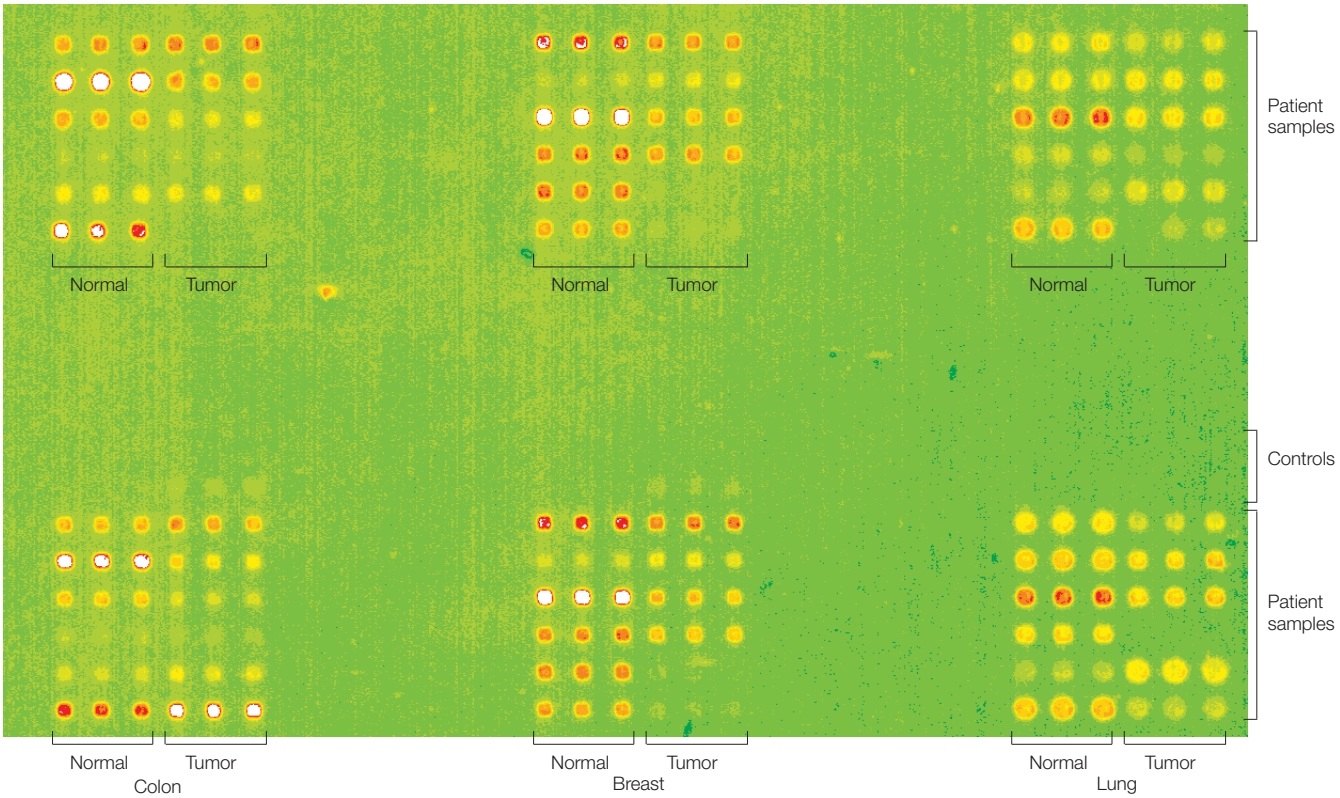

Fig. 1. False-color image of protein levels in a microarray of human clinical specimens. Normal and tumor lysates from six patients were arrayed and probed with an antibody to a circulating protein thought to correlate with differences in vascularization. Each row in a grid represents samples from a single patient. The first three spots in a row are from normal cells and the last three are from tumor cells. Upper and lower grids are duplicates of the same patient samples. The top two rows of the bottom grid consist of negative control spots to assess background noise of the assay.

development was achieved by incubating the slides in tetramethylbenzidine (TMB) peroxidase substrate (Sigma-Aldrich Co.), and the slides were subsequently scanned using an ArrayIt SpotWare colorimetric microarray scanning system (TeleChem International, Inc.).

Results and Discussion

Protein arrays were used to evaluate several criteria associated with the manufacture and use of this platform as a tool for cancer research. After slides were spotted, labeled, and imaged, false-color images were generated to reveal differential protein target content within each matched pair of samples. Figure 1 shows the differential abundance of a circulating protein marker in normal and tumor samples derived from multiple tissues and multiple patients. For example, in breast tumors, all normal samples displayed higher levels of the protein than the tumor samples. Spot size and deposition were within acceptable limits (10% CV) as was signal-to-noise ratio for colorimetric detection of protein biomarkers using immunological detection methods. Sensitivity using TMB was in the low picogram range.

In our laboratory, the BackTracker software feature that comes with the BioOdyssey Calligrapher miniarrayer adds a unique advantage over those offered in other array systems we have tried. Because we have to create our own source plates for the different protein array products we manufacture, the ability to easily predefine the robot printing program for each unique array layout requirement, which the BackTracker file system provides, is especially valuable.

This study demonstrates the successful use of the BioOdyssey Calligrapher miniarrayer for accurately and reproducibly printing protein arrays of complex biological samples derived from human tumors and normal tissues. The BackTracker software feature enhances our ability to rapidly redefine protein array templates and has significantly improved our product manufacturing capabilities. Rapid screening of multiple clinical specimens for protein biomarkers in a single assay in an easy-to-use platform not only is possible but also is a valuable first step in determining further analytical strategies.

References

Gulmann C et al., Proteomic analysis of apoptotic pathways reveals prognostic factors in follicular lymphoma, Clin Cancer Res 11, 5847–5855 (2005)

Krajewski S et al., Detection of multiple antigens on western blots, Anal Biochem 236, 221–228 (1996)

Nishizuka S et al., Proteomic profiling of the NCI-60 cancer cell lines using new high-density reverse-phase lysate microarrays, Proc Natl Acad Sci USA 100, 14229–14234 (2003)

For additional copies of this article, request bulletin 5480.

Rapid and Efficient Determination of Kinetic Rate Constants Using the ProteOn™ XPR36 Protein Interaction Array System

Vered Bronner, Tsafrir Bravman, Shai Nimri, and Kobi Lavie, Bio-Rad Laboratories, Inc., Gutwirth Park, Technion, Haifa 32000, Israel

Introduction

Surface plasmon resonance (SPR) optical biosensors are being used increasingly in a wide range of applications in basic biological research and pharmaceutical product development (Rich and Myszka 2005). We present here a significant advance in SPR biosensor technology: the ProteOn XPR36 protein interaction array system. The ProteOn XPR36 system incorporates a multichannel module and interaction array sensor chip for analysis of up to 36 independent protein interactions in a single injection step.

In a typical SPR biosensor experiment, a ligand is first immobilized onto a sensor chip surface and is then presented with an analyte in solution. The SPR biosensor detects the binding of the analyte to the ligand in real time and produces data on the association and dissociation kinetic rate constants of the reaction. When determining kinetic rate constants of a biomolecular interaction, a range of analyte concentrations is required to provide sufficient data for analysis. At the end of the binding step for a single analyte concentration, the ligand surface is normally regenerated before running the next analyte concentration.

In the ProteOn XPR36 protein interaction array system, there is no need to regenerate the ligand surfaces between samples because up to six analyte samples can be injected in parallel and in a single injection step. To do this, the multichannel module in the ProteOn XPR36 instrument first directs flow of six ligands (or one ligand under six different immobilization conditions) into six parallel channels across the sensor chip surface, and the ligands are then immobilized onto the chip surface. The multichannel module then directs the flow of analyte into another set of six parallel channels, which are orthogonal to the six ligand channels, to create a 6 x 6 ligand-analyte interaction array (Figure 1). Six sets of six sensorgrams are rapidly generated in a single analyte injection step. From these sensorgrams, detailed kinetic data can be obtained on the interaction of up to six analytes with up to six different ligands.

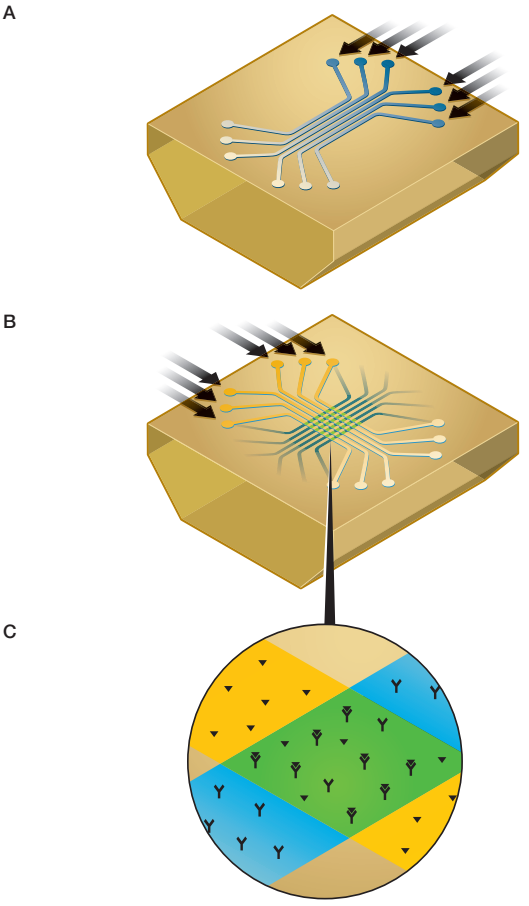

Fig. 1. Generation of the 6 x 6 ligand-analyte interaction array. A, six ligands are immobilized in six parallel ligand channels; **B**, six analyte samples are injected into six analyte channels orthogonal to the six ligand channels; **C**, detail of a single ligand-analyte interaction spot (green) showing the positions of the two interspot references (yellow).

In this tech note, we report the use of the ProteOn XPR36 system to determine the kinetic rate constants of the interaction between the human cytokine IL-2 and IL-2 antibody. Using "one-shot kinetics", six concentrations of IL-2 were presented in parallel across five different levels of immobilized IL-2 antibody (and one reference channel) to generate six sets of six sensorgrams that were then analyzed globally to yield kinetic constants in "one shot".

Methods

Instrumentation and Reagents

Experiments were performed using the ProteOn XPR36 protein interaction array system and one ProteOn GLC sensor chip. ProteOn phosphate buffered saline with 0.005% Tween 20, pH 7.4 (PBS/Tween) was used as running buffer throughout the experiments, and all experiments were performed at 25°C.

Immobilization of IL-2 Antibody

Mouse anti-human IL-2 antibody (ProteOn IL-2/IL-2 antibody pair) was immobilized on the ProteOn GLC sensor chip using the amine coupling reagents 1-ethyl-3-(3-dimethylaminopropyl)carbodiimide hydrochloride (EDAC) and *N*-hydroxysulfosuccinimide (sulfo-NHS) (ProteOn amine coupling kit). Five ligand channels on the carboxylated sensor chip surface were activated using five concentrations of EDAC and sulfo-NHS as follows: channel 1, 133 mM EDAC and 33 mM sulfo-NHS; channel 2, 88 mM EDAC and 22 mM sulfo-NHS; channel 3, 60 mM EDAC and 15 mM sulfo-NHS; channel 4, 40 mM EDAC and 10 mM sulfo-NHS; channel 5, 26 mM EDAC and 6.5 mM sulfo-NHS. Then, 180 µl IL-2 antibody (25 µg/ml in ProteOn acetate buffer, pH 4.5) was injected at a flow rate of 30 µl/min into the five activated channels and immobilized to five different levels dependent on the degree of surface activation in each channel. To deactivate remaining carboxyl groups, 1 M ethanolamine HCl, pH 8.5 (ProteOn amine coupling kit) was then injected into each channel. A sample of running buffer was included in each step for injection into the sixth channel, which was used as a reference channel.

IL-2 Binding

Human cytokine IL-2 (ProteOn IL-2/IL-2 antibody pair) samples were prepared at concentrations of 80, 40, 20, 10, 5, and 2.5 nM by serial dilution in PBS/Tween. Samples of each concentration (100 µl) were injected into the six analyte flow channels at a flow rate of 100 µl/min. The analyte injection step included a 1 min association phase followed by an 11.7 min dissociation phase in running buffer.

Sensorgram Analysis

The 36 sensorgrams were grouped into six sets of six, with each set corresponding to the interaction of the six IL-2 concentrations with each ligand (IL-2 antibody) density and reference channel. Each sensorgram set was processed for baseline alignment and referencing. Both a reference channel and interspot references were used for referencing.

The response unit (RU) measured with the ProteOn XPR system is equal to a change in refractive index of one part in 10^6 by use of a set of solutions with known refractive indices over the range of 1.33–1.37.

Results and Discussion

Uniformity of IL-2 Antibody Immobilization

The immobilization level of IL-2 antibody along the six interaction spots in a single ligand channel was uniform, with a CV of <3% for each of the five ligand channels (Table 1, column 1). This indicates that each protein interaction spot within a ligand channel is an equivalent immobilization surface. Therefore, the sensorgrams required for a detailed kinetic analysis can be generated from the interactions of six analyte concentrations with the six interaction spots along a single ligand channel.

Determination of Kinetic Rate Constants

Analytical curves describing a homogeneous 1:1 bimolecular reaction model were fit globally to each set of six sensorgrams (Figure 2). The residual error (χ^2) for each fit was <3% of the associated R_{max} value. The adjustable kinetic parameters for

Table 1. One-shot kinetic values for the IL-2/IL-2 antibody interaction. The equilibrium dissociation constant, K_D, was calculated from k_d/k_a. Values for ligand density are averages ± coefficient of variation (CV).

		IL-2 Cytokine (Analyte)							
	IL-2 Antibody (Ligand)	Interspot Reference Subtraction				Reference Channel Subtraction			
Channel	Ligand Density (RU)	k_a ($M^{-1}sec^{-1}$)	k_d (sec^{-1})	K_D (M)	R_{max} (RU)	k_a ($M^{-1}sec^{-1}$)	k_d (sec^{-1})	K_D (M)	R_{max} (RU)
1	2,823 ± 2.2%	7.73×10^5	1.19×10^{-4}	1.54×10^{-10}	147	7.98×10^5	1.30×10^{-4}	1.63×10^{-10}	148
2	2,053 ± 2.8%	7.57×10^5	1.32×10^{-4}	1.74×10^{-10}	119	7.96×10^5	1.36×10^{-4}	1.71×10^{-10}	120
3	1,702 ± 2.6%	8.08×10^5	1.33×10^{-4}	1.65×10^{-10}	102	8.87×10^5	1.30×10^{-4}	1.47×10^{-10}	102
4	1,468 ± 2.7%	8.00×10^5	1.34×10^{-4}	1.68×10^{-10}	90	7.86×10^5	1.36×10^{-4}	1.73×10^{-10}	91
5	1,368 ± 2.6%	7.78×10^5	1.33×10^{-4}	1.71×10^{-10}	84	8.84×10^5	1.31×10^{-4}	1.48×10^{-10}	85
6	Reference channel	—	—	—	—	—	—	—	—
Average	—	7.83×10^5	1.30×10^{-4}	1.66×10^{-10}	—	8.31×10^5	1.33×10^{-4}	1.60×10^{-10}	—
SD	—	2.07×10^4	6.30×10^{-6}	7.70×10^{-12}	—	5.00×10^4	3.13×10^{-6}	1.07×10^{-11}	—
CV (%)	—	2.64	4.84	4.63	—	6.02	2.36	6.66	—

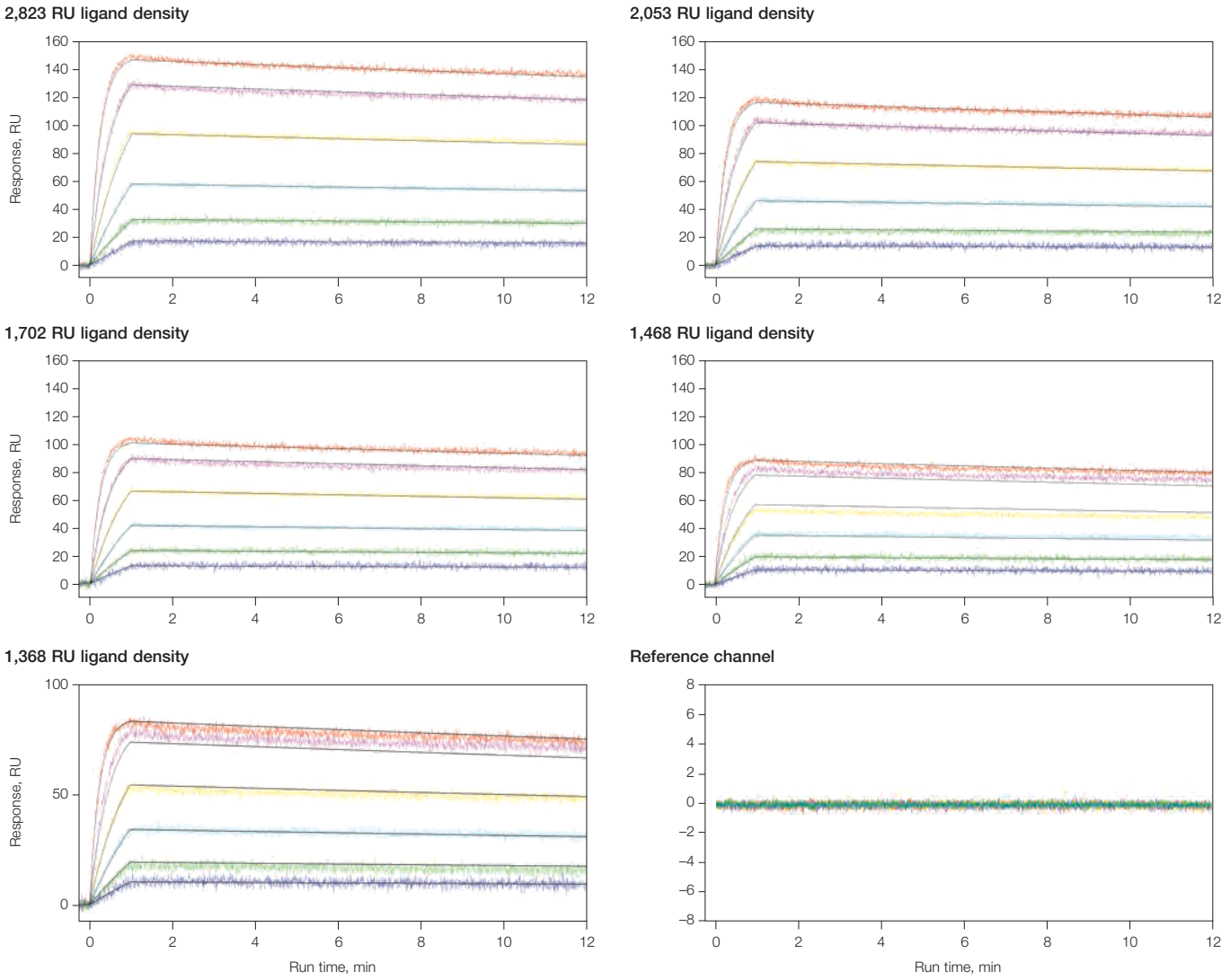

Fig. 2. One-shot kinetics for the IL-2 cytokine/IL-2 antibody interaction. Shown are the six sets of six sensorgrams generated in a single analyte injection step. Each set of six sensorgrams displays the responses from the six IL-2 cytokine concentrations (—, 80 nM; —, 40 nM; —, 20 nM; —, 10 nM; —, 5 nM; —, 2.5 nM) interacting with one immobilization level of IL-2 antibody. Sensorgrams are shown for the five levels of IL-2 antibody immobilization (ligand density) and the reference channel. Black lines represent the global fit of the sensorgrams to a 1:1 kinetic interaction model. See Table 1 for the kinetic constants derived from these data.

association (k_a), dissociation (k_d), and R_{max} for each IL-2 and IL-2 antibody sensorgram set were derived from the fitted curves and are shown in Table 1. The R_{max} values correlated well with the ligand immobilization levels (r = 99%).

Because each of the five experimental sensorgram sets provided acceptable fits, and because the interaction conditions were comparable, coefficients of variation (CVs) were calculated among these sets and were found to be in the range of 2–7% for the kinetic constants. Mass transport effects were estimated to be a minor contribution to the interaction by the consistency of the association rate constant at each ligand density (Table 1), which permitted the use of the five IL-2 antibody immobilization levels as replicates.

Reference Subtraction

In SPR experiments, referencing is needed to remove any contribution to the interaction response arising from differences in the refractive index of the sample solution vs. the refractive index of the running buffer (referred to as the "bulk effect"), and also from contributions due to drift and nonspecific binding. Referencing can be performed in two ways: by using a dedicated reference channel (for example, a channel that does not contain bound ligand) and by using interspot references.

A novel feature of the ProteOn XPR36 interaction array system is the ability to measure the SPR response in 42 interspot references. Interspot references are regions on the sensor chip situated between flow channels, and thus adjacent to both sides of

every interaction spot in the direction of analyte flow (Figure 1). During ligand immobilization, these interspot reference regions are not exposed to the activation or ligand solutions. However, during analyte binding, the interspot references are exposed to analyte flow, and because the interspot references do not have bound ligand, they can be used in place of a reference channel. The response of each interaction spot can be corrected by the average response from its two adjacent interspot references. Though any flow channel on the sensor chip may be used as a ligand or analyte reference channel, the inclusion of interspot references in the design of the ProteOn XPR36 system greatly increases its throughput and flexibility by allowing each flow channel to be used directly for interaction analysis.

Both referencing methods were used for the purpose of comparison, and the kinetic rate constants determined by both methods were nearly identical (Table 1). This demonstrates that results obtained using interspot references are equivalent to those obtained using a reference flow channel.

Finally, the %CV of the kinetic constants combined from samples prepared and analyzed independently on separate chips were in the range of <10%.

Conclusions

The capability of the ProteOn XPR36 protein interaction array system has been demonstrated for rapid and efficient determination of kinetic rate constants for protein interactions. Using one-shot kinetics, kinetic rate constants for the IL-2/IL-2 antibody interaction were determined from five replicate kinetic analyses in just 2 hr total instrument run time, including baseline stabilization and both the ligand immobilization and analyte binding injection steps.

A number of features of the ProteOn XPR36 protein interaction array system greatly increase the throughput, flexibility, and versatility of experimental design for protein-protein interaction analysis. In this experiment, the 6 x 6 interaction array was used to gain statistical confidence by treating the multiple interaction sets as replicates. In experimental situations where the interaction conditions are less known, the increased throughput can be used to immobilize ligand at different levels and to run analyte at different concentrations or in different buffers to rapidly find the optimal ligand immobilization and analyte binding conditions for the interaction under investigation.

In addition to the 6 x 6 interaction array, a number of other features enable the ProteOn XPR36 system to maximize throughput and flexibility for those experimental designs in which multiple ligand-analyte interactions are under investigation. The use of interspot references for sensorgram correction, which was validated in this study, lessens the need to dedicate a channel to referencing, and there is no need for regeneration (although the ligand surfaces can be regenerated for additional analytes, if needed). Because six analytes are run in parallel, kinetic analysis, K_D ranking, stability comparisons, epitope mapping, and other applications can be accomplished rapidly. The ProteOn XPR36 system represents a significant advance in SPR biosensor technology, and provides increased throughput and flexibility in experimental design.

Reference

Rich RL and Myszka DG, Survey of the year 2004 commercial optical biosensor literature, J Mol Recognit 18, 431–478 (2005)

For additional copies of this article, request bulletin 3172.

Target Expression and Target Modulation Studies in Patient-Derived Tumor Xenografts Using a Bank of Protein Lysates

Martina Maurer, Andreas Wortmann, André Korrat, Heike Legrand, Julia Schüler, Sandra Kissel, Niko Bausch, Thomas Metz, and Heinz-Herbert Fiebig,
Oncotest GmbH, Institute for Experimental Oncology, D-79108 Freiburg, Germany

Introduction

In this tech note, we present an efficient method that facilitates the preclinical analysis of antitumor compounds. By using specialized human tumor models and multiplex bead suspension assays, we are able to decide which tumor models to use for preclinical profiling of anticancer agents as well as identify biomarkers for specific drug response or resistance.

Methods

Protein Tumor Lysate Bank

By directly transplanting patient tumors subcutaneously into immune-compromised nude mice, more than 400 solid tumors, including all major human tumor types, have been established in serial passage (Fiebig et al. 1992, Fiebig and Burger 2001). At Oncotest, we have generated a protein tumor lysate bank consisting of 150 tumor models (Table 1).

Table 1. Xenografts selected for the protein tumor lysate bank (n = 150).

Bladder	4	Lymphoma	4	Pancreas	4
Colon	19	Mammary	14	Pleuramesothelioma	2
Gastric	4	Melanoma	12	Prostate	5
Head and neck	4	Non-small cell lung cancer (NSCLC)	33	Sarcomas	4
Kidney	6			Uterus	5
Leukemias	5	Small cell lung	6	Others	8
Liver	3	Ovarian	8		

Multiplex Bead Suspension Assays

Bead suspension assays are flexible bioassay systems that allow the parallel detection and quantitation of many targets in a single sample. For example, we can measure up to 28 cytokines and chemokines or 7 phosphorylated signal transduction proteins simultaneously. In a typical multiplex bead suspension assay, a target protein is captured from a crude cell lysate, tissue lysate, or serum with bead-bound antibodies. The total target protein amount and/or its phosphorylation status is quantitated with a secondary biotinylated antibody followed by an incubation step with streptavidin-phycoerythrin to complete a sandwich immunoassay. In this study, we used Bio-Rad's Bio-Plex™ multiplex suspension array system and Oncotest xenograft lysates (Figure 1).

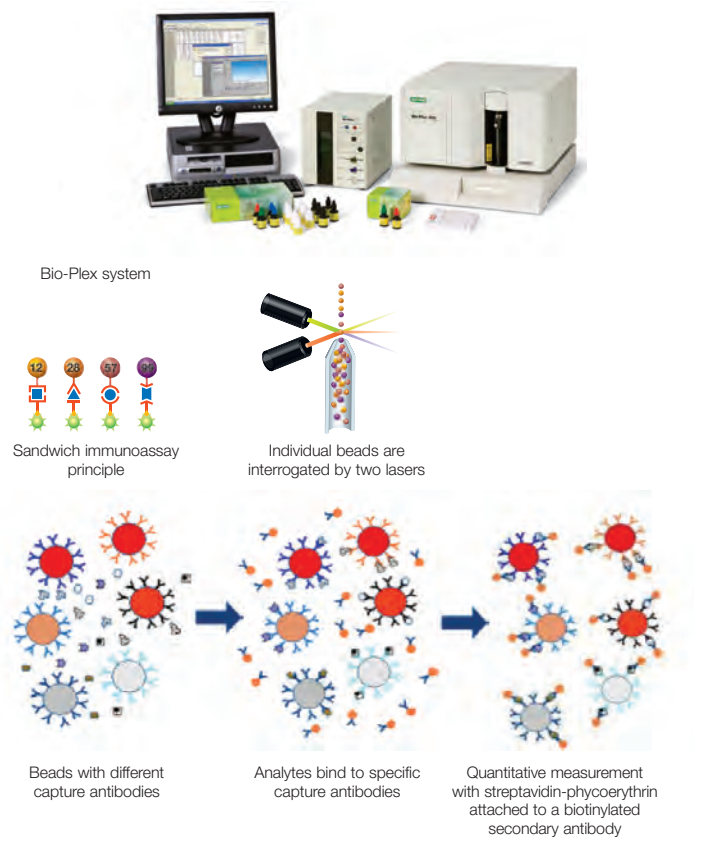

Fig. 1. Multiplex bead suspension assay test principle. The Bio-Plex multiplex system and Oncotest xenograft lysates (n = 150) were used to determine total target amount and phosphorylation status.

Results and Discussion

Expression Profiling

Multiplex bead suspension assays (Table 2) were used to determine the expression and phosphorylation state of a multitude of molecular markers involved in signal transduction, cell cycle, apoptosis, and so on. The expression profiles allowed the selection of optimal tumor models for the in vivo testing of novel anticancer agents (Figure 2). Furthermore, we used the complete molecular profiles to identify biomarkers predictive for drug response or resistance.

Target Monitoring

Another application of the multiplex bead suspension assays was the monitoring of target expression and activity (e.g., phospho-EGFR) during therapy experiments in tumor-bearing nude mice (Figure 3).

Table 2. Multiplex bead assays available at Oncotest as of February 2006. Highlighted assays are developed and manufactured at Bio-Rad.

Phosphorylated Signal Transduction Proteins
Phospho-Akt/PKB (Ser^{473})
Phospho-ATF-2 (Thr^{71})
Phospho-c-Jun (Ser^{63})
Phospho-c-Kit
Phospho-c-Met
Phospho-CREB (Ser^{133})
Phospho-EGF receptor
Phospho-ERK/MAP kinase 1/2 (Thr^{185}/Tyr^{187})
Phospho-GSK-3α/β (Ser^{21}/Ser^{9})
Phospho-HSP27 (Ser^{78})
Phospho-IκB-α (Ser^{32})
Phospho-IRS-1
Phospho-JNK/SAPK1 (Thr^{183}/Tyr^{185})
Phospho-Jun (Ser^{73})
Phospho-Lck
Phospho-NF-κB (Ser^{536})
Phospho-p38 MAPK (Thr^{180}/Tyr^{182})
Phospho-p53 (Ser^{15})
Phospho-p70 S6 kinase (Thr^{421}/Ser^{424})
Phospho-p90RSK (Thr^{359}/Ser^{363})
Phospho-PDGF receptor a
Phospho-PRAS40 (Thr^{245})
Phospho-Rb (Ser^{249}/Thr^{252})
Phospho-Rb (Thr^{821})
Phospho-RSK1/MAPKAP kinase 1a (Ser^{380})
Phospho-STAT1 (Tyr^{701})
Phospho-STAT2
Phospho-STAT3 (Tyr^{705})
Phospho-STAT3 (Ser^{727})
Phospho-STAT5A/B (Tyr$^{694/699}$)
Phospho-Tau (Ser^{199})
Phospho-Tau (Thr^{181})
Phospho-TrkA (Tyr^{490})

Total Signal Transduction Proteins
Total Akt/PKB
Total ATF-2
Total active β-catenin
Total c-Kit
Total c-Jun
Total CREB
Total EGF receptor
Total ERK/MAP kinase 1/2
Total ERK2
Total HSP27
Total IκB-α
Total IRS-1
Total JNK/SAPK1
Total Lck
Total p38 MAPK
Total p53
Total p70 S6 kinase
Total p90RSK
Total Rb
Total STAT1
Total STAT3
Total Tau

Apoptosis-Associated Proteins
Active caspase 3
Bcl-2
Cleaved PARP
Single-stranded DNA

Transcription Factors
AP-2
CREB
EGR
HIF
NF1
NF-κB
NFAT
PPAR
SRE
YY1

Matrix Metalloproteins
MMP-1
MMP-2
MMP-3
MMP-7
MMP-8
MMP-9
MMP-12
MMP-13

Death Receptors
DR5
TNF-RI
TNF-RII

Cytokines and Chemokines
Eotaxin
GM-CSF
G-CSF
IL-1α
IL-1β
IL-2
IL-3
IL-4
IL-5
IL-6
IL-7
IL-8
IL-10
IL-12 (p40)
IL-12 (p70)
IL-13
IL-15
IL-17
Interferon-α2
Interferon-γ
IP-10
MCP-1
MIP-1α
MIP-1β
RANTES
TNF-α
TNF-β

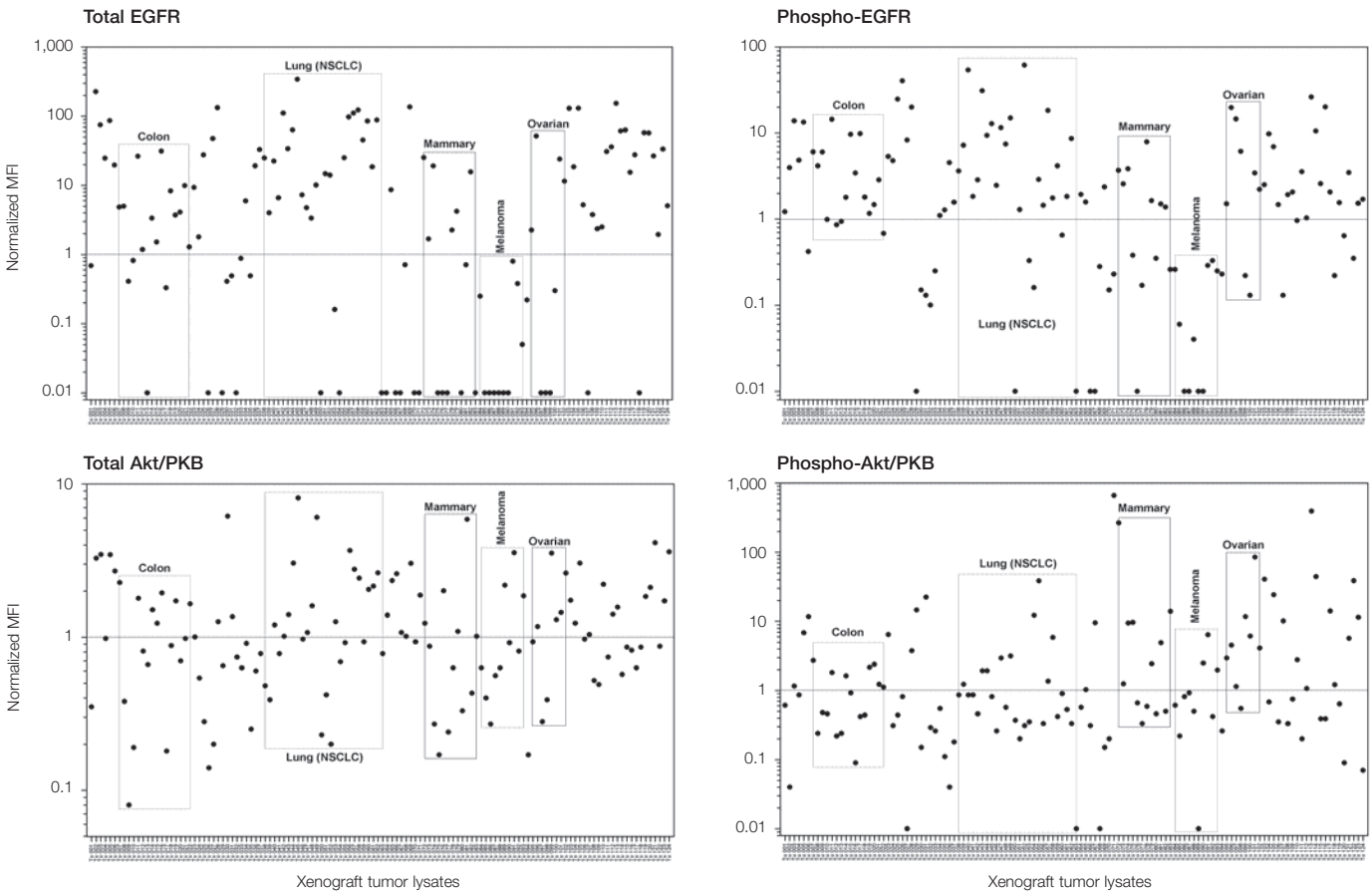

Fig. 2. Expression profiling of total proteins and phosphoproteins in 124 human tumor models. Upper panels, total and phospho-EGFR amounts; lower panels, Akt/PKB amounts. Each parameter was measured with the Bio-Plex system, and the black line shows the geometric mean value over all tumors. Tumors above the line exhibit enhanced protein expression or phosphorylation, respectively. These xenografts are suitable tumor models for target-directed in vivo studies.

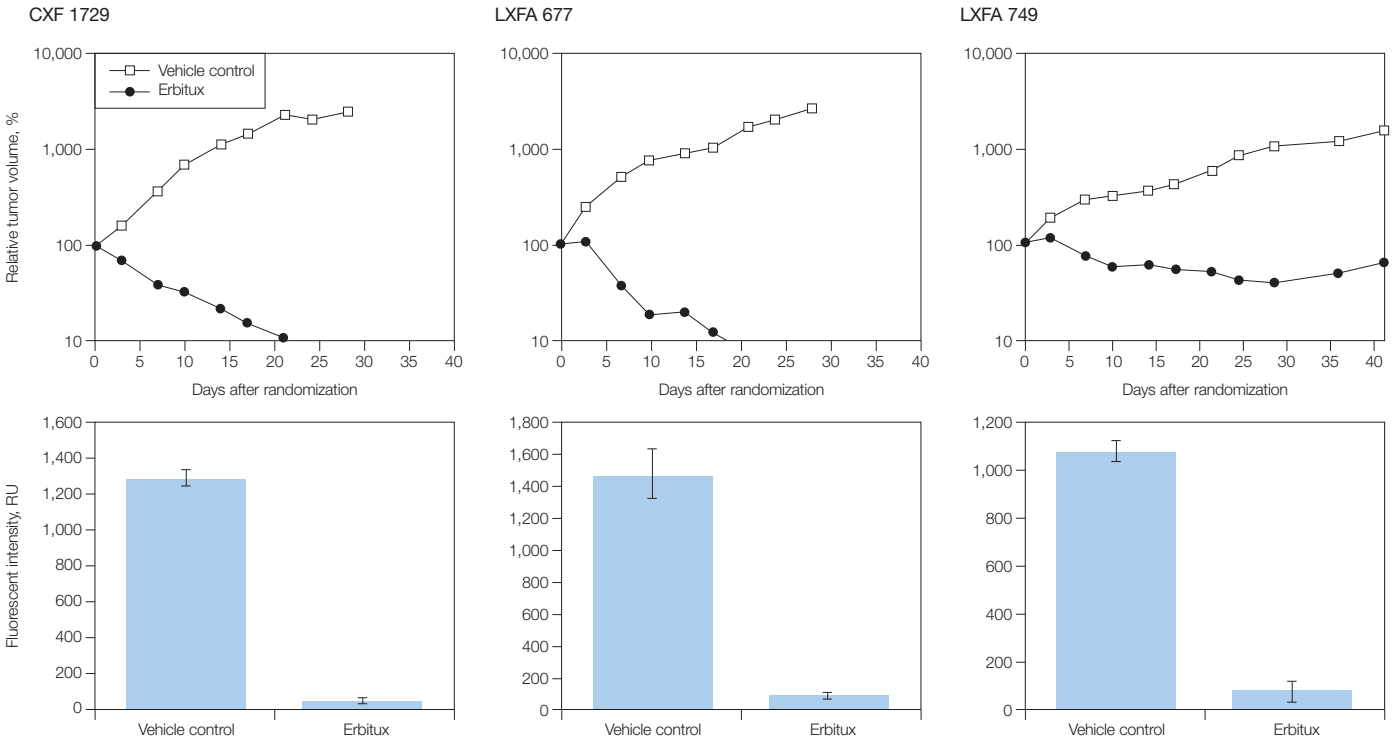

Fig. 3. Target monitoring for EGFR-inhibitory monoclonal antibody Erbitux in three sensitive tumor xenografts. Upper panels show tumor volume inhibition over time after intraperitoneal treatment with Erbitux on days 1, 8, and 15 at 30 mg/kg. Lower panels show the drop of EGFR phosphorylation 24 hr after administration of a single dose of Erbitux. CXF = colon carcinoma xenograft Freiburg; LXFA = lung adenocarcinoma xenograft Freiburg.

Conclusions

The detailed molecular characterization of Oncotest's tumor collection allows an optimal choice of tumor models for the preclinical profiling of promising new anticancer agents. This approach accelerates and improves the preclinical evaluation of novel target-directed compounds. In addition, the identification of biomarkers specific for drug response or resistance can be used as a diagnostic tool to determine the most promising individual therapy for cancer patients.

Acknowledgement

We thank Nicole Gollmitzer (Bio-Rad, Germany) for excellent technical advice.

References

Fiebig H-H et al., Combined in vitro/in vivo test procedure with human tumor xenografts for new drug development, Contrib Oncol 42, 321–351 (1992)

Fiebig H-H and Burger AM, Human tumor xenografts and explants, pp 113–137 in Teicher BA (ed), Tumor Models in Cancer Research, Humana Press, Totowa, NJ (2001)

For additional copies of this article, request bulletin 5301.

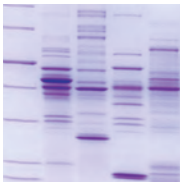

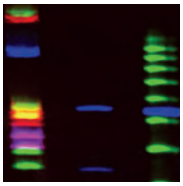

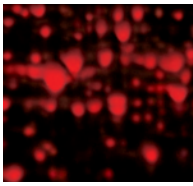

Great images are only part of the picture.

Bio-Rad's tradition of excellence and commitment to your success make the picture complete.

We Share Your Vision

Through decades of cooperation with our customers across the globe, Bio-Rad has refined the tools you use every day. Our R&D scientists use these same tools to ensure effective detection, analysis, and downstream processing of scientific data. We understand the critical importance of application-specific imaging and analysis to your success.

Bio-Rad's Molecular Imager® systems provide the sensitivity, high resolution, and dynamic range vital to optimize your workflows. Whatever your goals — from verification of clones to PCR, from total protein detection to multiplex fluorescent tagging — Bio-Rad has an imaging system that's just right for you.

Bio-Rad imaging — more than 50 years of science in every imaging system. For more information, visit us on the Web at **www.bio-rad.com/imaging/**

Molecular Imager systems — your vision ahead.

The Life Science LSIA 2006 Industry Awards

Bio-Rad Laboratories, Inc.
2006 Award Winner —
Best Image Analysis Systems

Practice of the polymerase chain reaction (PCR) may require a license.

Visit us on the Web at **discover.bio-rad.com**
Call toll free at 1-800-4BIORAD (1-800-424-6723);
outside the US, contact your local sales office.

BIO-RAD

Amplification
- Amplification product catalog supplement, US (bulletin 5435)
- Convenient multiplex PCR assays with iQ™ multiplex powermix (bulletin 5438; PDF only)
- iCycler® thermal cycler modules and upgrades flier (bulletin 2653)
- Real-time PCR quantitation of *Leptospira* in a hamster model (bulletin 5372; PDF only)

Gene Transfer
- Gene Pulser Xcell™ system product information sheet (bulletin 5445)
- Helios® gene gun product information sheet (bulletin 5446)
- Biolistic PDS-1000/He™ system product information sheet (bulletin 5447)
- MicroPulser™ electroporator product information sheet (bulletin 5448)
- siLentMer™ Dicer-substrate siRNA duplexes product information sheet (bulletin 5375)

Microarray Products
- Proteomic analysis of tumor biomarkers in human clinical specimens using the BioOdyssey™ Calligrapher™ miniarrayer (bulletin 5480)
- Genotyping by arrayed primer extension (APEX) using the BioOdyssey Calligrapher miniarrayer (bulletin 5392)

Sample Preparation
- First-dimension separation with the MicroRotofor™ cell prior to SDS-PAGE and LC-MS/MS analysis (bulletin 5451)

Chromatography
- A method for rapid, large-scale removal of albumin and IgG from human serum using the BioLogic DuoFlow™ chromatography system (bulletin 5334)
- Profinity™ IMAC resin: an optimal support for His-tagged protein purification (bulletin 5456)
- Process-scale chromatography brochure (bulletin 5488)

Electrophoresis
- Proteomweaver™ 2-D analysis software brochure (bulletin 5400)

Multiplex Suspension Array Technology
- Bio-Plex™ phosphoprotein detection flier (bulletin 5482; PDF only)
- Bio-Plex phosphoprotein detection data sheet (bulletin 5483)
- Target expression and target modulation studies in patient-derived tumor xenografts using a bank of protein lysates (bulletin 5301)
- Lysate preparation for Bio-Plex phospho-histone H3 assay (bulletin 5377; PDF only)

Protein Interaction Analysis
- ProteOn™ system ordering information sheet (bulletin 5409)*
- ProteOn XPR36 hardware product information sheet (bulletin 5413)*
- ProteOn protocol development kits product information sheet (bulletin 5410)*
- ProteOn sensor chips product information sheet (bulletin 5404)*
- ProteOn XPR36 application guide product information sheet (bulletin 5412)*
- ProteOn XPR36 protein interaction array system video tour (bulletin 5465)*

Bioinformatics
- Proteomweaver™ 2-D analysis software brochure (bulletin 5400)

E-Commerce
- E-commerce for customers and businesses brochure (bulletin 5314)

* Included in protein interaction information folder (bulletin 5434A)

iProof™ High-Fidelity DNA Polymerase

A Powerful Bond

Bio-Rad's unique iProof high-fidelity DNA polymerase delivers unsurpassed speed and fidelity, with higher yields and fewer reaction failures, for all your PCR needs.

- **Fidelity — novel proofreading enzyme is the most accurate thermostable polymerase (52-fold more accurate than *Taq*)**
- **Speed — increased processivity dramatically reduces extension steps (15–30 sec/kb) and overall reaction times**
- **Length — large fragments (up to 37 kb) amplified in less time and with less enzyme (0.25–1 unit/reaction)**

For more information, visit us on the Web at **www.bio-rad.com/iproof/**

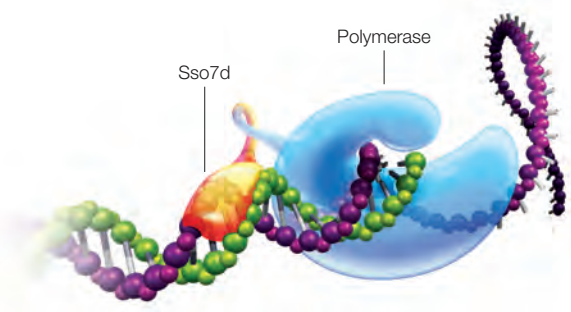

Fusing the double-stranded DNA binding protein Sso7d to iProof gives it a powerful sliding grip on the replicated DNA.

Practice of the polymerase chain reaction (PCR) may require a license.

Visit us on the Web at **discover.bio-rad.com**
Call toll free at 1-800-4BIORAD (1-800-424-6723);
outside the US, contact your local sales office.

BIO-RAD

One just right for you.

Find the cycler that best reflects your needs among the full line of Bio-Rad amplification products.

Bio-Rad is committed to providing you with the best tools for your PCR needs. This dedication is proven by our history of innovation, quality, and regard for researchers' needs.

- Flexible, space-saving dual blocks and multi-bay instruments
- The only modular real-time cycler upgrade with a thermal gradient; choose from 1 to 5 colors
- Innovative enzymes that work where others fail
- PCR tubes, plates, and sealers for any application
- Dedicated technical support by experienced scientists

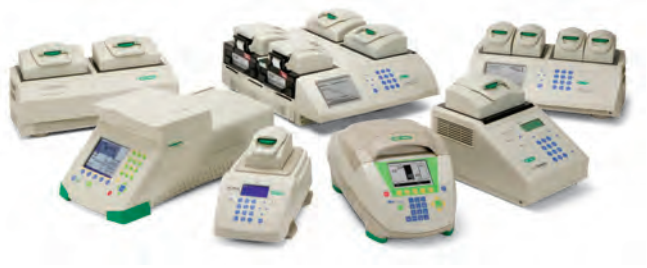

Bio-Rad offers the most complete line of thermal cyclers anywhere.

For more information, visit us on the Web at **www.bio-rad.com/genomics/**

Visit us on the Web at **discover.bio-rad.com**
Call toll free at 1-800-4BIORAD (1-800-424-6723);
outside the US, contact your local sales office.

BIO-RAD